Marine Pollution Bulletin 224 (2026) 119080

Contents lists available at ScienceDirect

Marine Pollution Bulletin

journal homepage: www.elsevier.com/locate/marpolbul

Climatic and nutrient drivers affect long-term phytoplankton temporal trends in coastal lagoons

Aurore Moulin [a,c,f,*,1], Béatrice Bec [b,1], Olivier Boutron [c], Valérie Derolez [d], Marie Garrido [e], Vanina Pasqualini [a], Nathalie Malet [f]

[a] UMR SPE CNRS Università di Corsica Pasquale Paoli, 20250, Corte, France
[b] MARBEC, Univ Montpellier, CNRS, Ifremer, IRD, Montpellier, France
[c] Tour du Valat Research Institute, Le Sambuc, 13200, Arles, France
[d] MARBEC, Univ Montpellier, CNRS, Ifremer, IRD, Sète, France
[e] Environmental Agency of Corsica, 14 Avenue Jean Nicoli, 20250, Corte, France
[f] Ifremer LERPAC/CO, 20600, Bastia, France

ARTICLE INFO

Keywords:
Climatic and nutrient drivers
Coastal lagoons
Long-term dynamics
Phytoplankton community
Site-specific responses

ABSTRACT

Understanding how climate influences phytoplankton dynamics is crucial for anticipating temporal trends and cascading consequences on ecosystem functioning under climate change. This study explores long-term dynamics in contrasted Mediterranean lagoons and investigates the effects of climatic (air temperature, rainfall, wind speed) and nutrient (inorganic nutrient concentrations) drivers on phytoplankton chlorophyll *a*, abundances, and pigment composition. 17 years of summer monitoring were analyzed using univariate trend tests and multivariate approaches to highlight changes and to disentangle the contributions of abiotic factors to phytoplankton variability. Our results revealed contrasts among lagoons in physicochemical conditions and phytoplankton community, which strongly structured their temporal trends. Climatic drivers significantly influenced phytoplankton, but their importance was context-dependent. In nutrient-enriched systems, phytoplankton dynamics were primarily controlled by inorganic nutrient concentrations, while climatic effects were weak by comparison. Conversely, in nutrient-poor systems, climatic signals became more visible and influential: wind events were associated with higher chlorophyll *a*, warmer conditions with increases in phycoerythrin-rich picocyanobacteria, and rainfall with higher picoeukaryote abundances, potentially through indirect effects on water column stability and nutrient and light availability. However, under nutrient limitation, abundances remained low and dominated by small cells, suggesting that nutrient control exerts the strongest influence on phytoplankton, which may explain why nutrient control tends to mask diffuse climatic signals. Yet, climate change modulates physicochemical patterns and may progressively shape lagoon functioning. This study emphasizes the need to account for lagoon features and vulnerabilities, and supports adaptive and site-specific management strategies to safeguard coastal lagoons under future changes.

1. Introduction

Coastal lagoons provide ecological and socio-economic ecosystem services, including carbon sequestration, contributing to climate change mitigation (Newton et al., 2018; Guzmán et al., 2023). However, their functioning is complex, driven by interactions of physical, chemical and biological processes leading to significant internal spatiotemporal variability in response to environmental changes (Tagliapietra et al., 2009; Pérez-Ruzafa et al., 2011). Climate change is characterized by a global rise in temperatures, projected to reach 1.8–4.4 °C by the end of the 21st century, along with altered seasonal precipitation patterns with drier summers and wetter winters (Levang and Schmitt, 2015; Rodrigues et al., 2021; IPCC, 2023), and a higher frequency and intensity of extreme weather events such as heat waves, torrential rainfall, or storms (Da Costa et al., 2022). Exposed to influences from the atmosphere, ocean and land (Tagliapietra et al., 2009; Rodrigues et al., 2021), coastal lagoons are transitional systems especially vulnerable to ongoing climatic threats (Newton et al., 2018), justifying their designation as

* Corresponding author at: UMR SPE CNRS Università di Corsica Pasquale Paoli, 20250, Corte, France.
E-mail address: moulin_a@univ-corse.fr (A. Moulin).
[1] Equal contribution.

https://doi.org/10.1016/j.marpolbul.2025.119080
Received 25 July 2025; Received in revised form 25 November 2025; Accepted 27 November 2025

"sentinels of climate change" (Eisenreich et al., 2005; Guzmán et al., 2023). Heatwaves, heavy rainfall and wind events can significantly affect lagoon hydrology (Jiang et al., 2022; Tuchkovenko et al., 2023; Macias et al., 2025) and physicochemical conditions, including salinity, water temperature, oxygenation and nutrient fluxes (Shalby et al., 2020; Rodrigues et al., 2021; Da Costa et al., 2022). Mediterranean coastal lagoons are particularly vulnerable, as they are typically shallow, semi-enclosed, and subject to anthropogenic pressures within a region considered a global warming hotspot (Giorgi, 2006; Mediterranean Wetlands Observatory (MWO), 2018). These characteristics exacerbate their reactivity to climate signals (Bird, 2011; Lopez et al., 2019), making them sensitive and key systems to detect climate effects on ecosystem functioning. Climate change can influence management challenges (Jeppesen et al., 2007; Stefanova et al., 2019), including watershed use (Rodrigues et al., 2021), lagoon-sea connectivity and eutrophication control (La Jeunesse et al., 2015; Chen et al., 2023), underscoring the urgency of targeted mitigation strategies.

These environmental changes also affect lagoon biodiversity, particularly the phytoplankton (Lopes et al., 2019; Pesce et al., 2018). As primary producers and key components of aquatic ecosystems, phytoplankton sustain trophic networks, drive primary productivity and regulate biogeochemical cycles (Field et al., 1998). Their seasonal and interannual dynamics are mainly influenced by nutrient availability, salinity, water temperature, water column stability, light penetration, and grazing (Cloern, 1999; Pomati et al., 2020; To et al., 2025), all of which are modulated by climatic conditions (Berger et al., 2006; Tuchkovenko et al., 2023). Due to their high growth rates, phytoplankton communities can respond within days to environmental fluctuations (Field et al., 1998; Jiang et al., 2022; Grossi et al., 2024), and their growth potential may even increase with global warming scenarios (Vanselow et al., 2022). Phytoplankton communities are also highly diverse, with contrasting ecological requirements (Cloern, 1999; Bec et al., 2011). This combination of reactivity and diversity makes phytoplankton both sensitive and informative bioindicators, well-suited for assessing water quality (Sathicq et al., 2017) and detecting climate-induced changes (Lopes et al., 2019). While eutrophication-related phytoplankton trajectories have been widely studied (Bec et al., 2011; Leruste et al., 2016; Derolez et al., 2019; Ouaissa et al., 2023), long-term climate change responses remain less understood and more complex to detect, due to the difficulty of disentangling climatic effects from nutrient influences, which co-occur, interact (Stefanova et al., 2019; Guzmán et al., 2023), and generate group-specific responses (Xu et al., 2022). Climate change, by modifying both physical-chemical conditions and biological processes (Winder and Sommer, 2012; Da Costa et al., 2022), is expected to reshape phytoplankton trajectories through shifts in biomass, bloom dynamics and community composition (Valenti et al., 2016; Pesce et al., 2018; Bi et al., 2021; Sabater et al., 2023). Some predict an overall increase in total biomass under warmer and more illuminated conditions (Rodrigues et al., 2021; Minicheva et al., 2018; Talavera et al., 2024). Other research suggests that warming may modify interactions between temperature, nutrient levels, and grazing pressure, thereby intensifying zooplankton control and potentially shifting the relative contribution of phytoplankton size classes (Pomati et al., 2020; Bi et al., 2021). Rising temperatures can also reinforce water column stratification, limiting vertical nutrient mixing and promoting nutrient limitation in surface waters (Da Costa et al., 2022; Vereshchaka et al., 2023), which leads to a decline in total phytoplankton biomass. Warming may enhance internal nutrient recycling from sediments, potentially favoring certain phytoplankton groups (Pesce et al., 2018). Shifts toward stress-tolerant species adapted to warming, salinity, or hypoxia are increasingly predicted (Oviatt, 2004; Wang et al., 2025). The resulting modification of nutrient-light balance with climate change may favor cyanobacteria over diatoms (Pesce et al., 2018; Jiang et al., 2022; Wang et al., 2025), leading to detectable shifts in pigment contributions and group abundances. In Mediterranean lagoons, Bec et al. (2011) reported an increase in phycoerythrin-rich picocyanobacteria under warming, a trend supported by the high physiological plasticity and clade diversity of the picocyanobacterial taxa, enabling adaptation to fluctuating temperature, salinity, and nutrient conditions (Doré et al., 2022). In parallel, episodic events such as rainfall and wind can stimulate phytoplankton development through water column mixing, nutrient resuspension, or increased external inputs (Goberville et al., 2010; De Oliveira et al., 2023; Grossi et al., 2024; Wang et al., 2025). Altered precipitation regimes can also influence the annual patterns of nutrient availability, potentially modifying phytoplankton community composition (Pesce et al., 2018). These phytoplankton shifts may cause cascading impacts on zooplankton (To et al., 2025) and benthic communities (Pasqualini et al., 2017), food web dynamics (Goberville et al., 2010; Lopez et al., 2019), ultimately affecting the resilience and ecosystem services of lagoons (Pesce et al., 2018).

However, few studies have explicitly disentangled the influence of climatic versus nutrient drivers, and even fewer have done so using long-term datasets. Here, using a 17-year summer dataset from four contrasting Mediterranean coastal lagoons, we investigate phytoplankton dynamics to identify temporal trends, reveal the main abiotic drivers, and distinguish the relative influences of climatic and nutrient forcing. This question is especially relevant in these lagoons, where existing monitoring data have only been partially exploited, and distinct characteristics provide an opportunity to test whether ecological responses are site-specific. By combining multiple phytoplankton metrics (chlorophyll *a*, size-structured abundances, and pigment composition) with linear and nonlinear statistical approaches and carefully designed temporal windows to capture local climatic effects, this study provides detailed insights into the taxonomic and functional patterns of phytoplankton responses to environmental changes.

We hypothesize that climatic drivers influence phytoplankton mainly through impacts on community composition. Air temperature may favor warming-adapted taxa (picocyanobacteria, dinoflagellates), while rainfall and wind, by enhancing nutrient availability, may promote nutrient competitive groups such as diatoms or picoeukaryotes. Climate change may thus drive reorganizations within size classes rather than marked shifts in total biomass, with site-specific responses depending on lagoon features. This study aims to anticipate future ecological trajectories and to support the development of adaptive and targeted management strategies for coastal lagoons.

2. Materials and methods

2.1. Study sites

Four contrasted Mediterranean coastal lagoons are investigated in our study, located along the eastern coast of the Corsican Island (Biguglia, Palo, Diana, Urbino; Fig. 1). All are connected to the Mediterranean Sea through sea channels that show a progressive tendency toward closure (Orsoni et al., 2001; Garrido et al., 2016). These lagoons differ in hydromorphology and salinity status (Table 1). Biguglia and Palo are shallow systems, whereas Diana and Urbino, with a tectonic origin, are deeper. Biguglia is meso-polyhaline, with a large size and a northern basin influenced by seawater exchanges and a southern basin receiving freshwater inputs from the watershed and the Golo River (via the Fossone Canal). This north-south hydrological gradient results in the distinction between two separate basins (Fig. 1). Diana and Urbino maintain a relatively stable euhaline state that tends toward hyperhalinity. Palo is smaller and more confined, with strong seasonal fluctuations ranging from polyhaline conditions during the rainy season to hyperhaline states in summer. Human activities also vary among lagoons (Table 1). Biguglia has the largest and most urbanized watershed. Diana and Urbino have smaller watersheds mainly covered by vineyards. Diana supports an active shellfish farming, while Urbino hosted fish farming until the 2000s (Ligorini et al., 2022a). Palo's watershed is surrounded by wetlands and is moderately urbanized, with an airbase and a commercial area. All the lagoons support fishing activity (AERMC

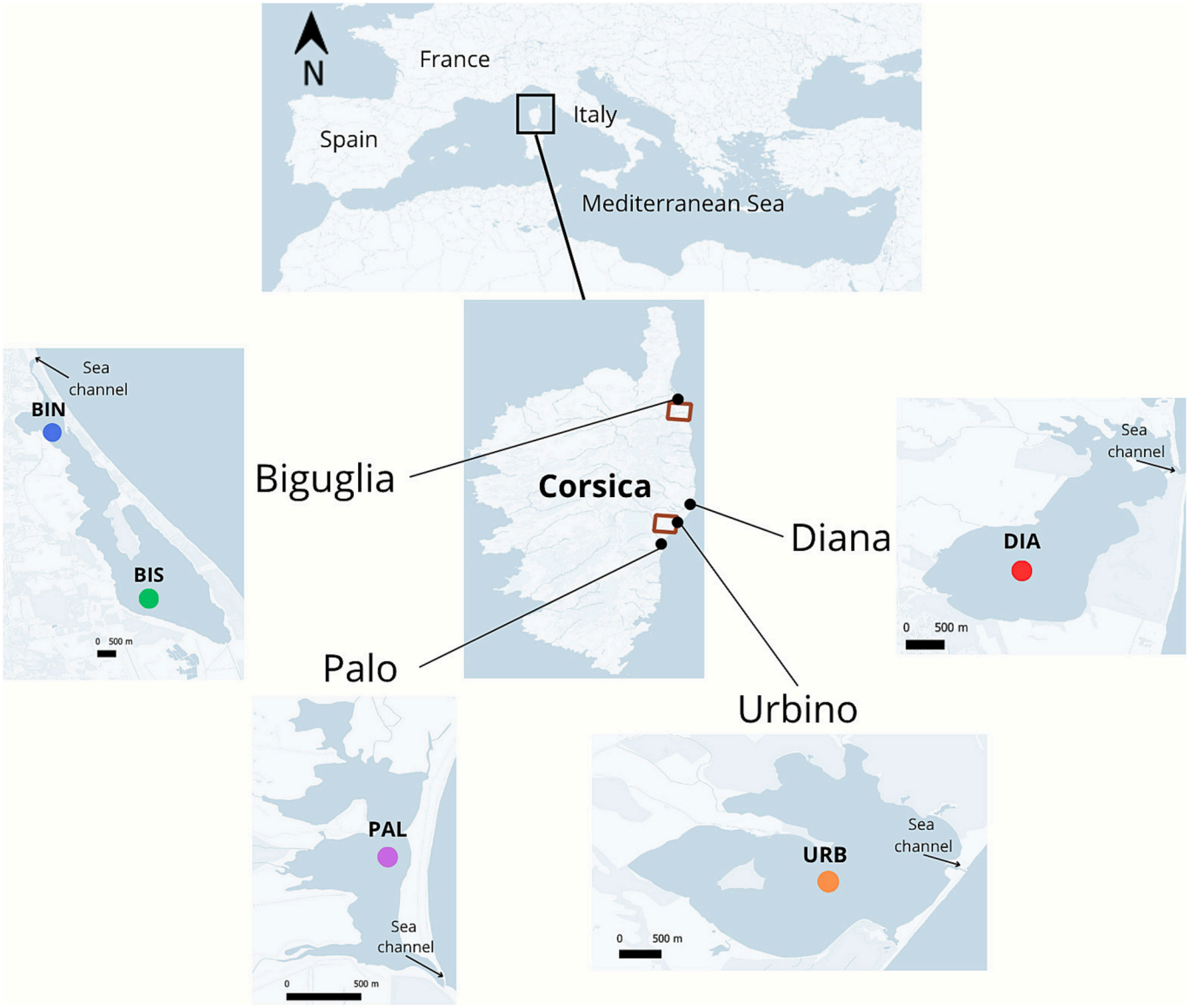

Fig. 1. Locations (black dots) of the four studied lagoons along the Corsican coastline. The locations of the five sampling stations across the study lagoons are also represented: BIN and BIS in Biguglia (blue and green points), DIA in Diana (red point), URB in Urbino (orange point), and PAL in Palo (purple point). The two brown rectangles correspond to the climatic grid cells used in the analysis (North cell and South cell). (For interpretation of the references to colour in this figure legend, the reader is referred to the web version of this article.)

(Agence de l'eau Rhône Méditerranée Corse), 2021).

2.2. Long-term data collection

The long-term data series (2007–2023) on phytoplankton and physicochemical parameters were obtained from the Lagoon Monitoring Network (LMN), the OBSLAG program and under the Water Framework Directive. Sampling was conducted at five stations in total (Fig. 1). In Biguglia Lagoon, two stations were monitored: BIN in the north and BIS in the south. In Diana, Urbino and Palo, one central station was sampled (DIA, URB, PAL). Data were collected each year and once per month during the summer period (June, July, August). This monitoring period was targeted because it corresponds to the peak of primary productivity in Mediterranean lagoons and provides a critical window to assess their eutrophication status (Souchu et al., 2010; Bec et al., 2011).

2.2.1. Physicochemical data

Physicochemical monitoring combined in situ measurements with WTW LF 197 field sensor (precision ±0.5 %) for salinity (SALI, PSU), water temperature (TEMP, °C), turbidity (TURB, NTU), dissolved oxygen (O2, mg L − 1) (Bec et al., 2011); and laboratory analyses of surface water samples (0–1 m) collected in 2 L polypropylene bottles for dissolved inorganic phosphorus (DIP, µmol L^{-1}), dissolved inorganic nitrogen (DIN = NO3+ NO2+ NH4, µmol L^{-1}), total nitrogen (NT, µmol L^{-1}) and total phosphorus (PT, µmol L^{-1}). Subsamples of 100 mL were filtered through Whatman GF/F membranes (0.7 µm) and analyzed with segmented flow analyzers to determine dissolved inorganic nutrients, while NT and PT were quantified from unfiltered samples, following the protocol described by David et al. (2019).

2.2.2. Climatic data

Climatic data were extracted from the SAFRAN reanalysis system, which provides daily values on an 8 × 8 km^2 grid (Vidal et al., 2010). To capture local-scale climate variability, two grid cells were selected based on their proximity to the study sites: one nearest Biguglia (42°54′00″ N, 9°48′63″ E; named North cell), and another nearest Diana, Urbino, and

Table 1
Main characteristics of the five study sites, including lagoon morphology, summer trophic status, summer chlorophyll *a*, annual mean, minimum, and maximum for salinity and water temperature for the period 2023/2024, freshwater and seawater exchange regimes, watershed surface area, and detailed human activities. Data were compiled from the following sources: (1) *Limnol. Oceanogr.* (1958), (2) Orsoni et al., 2001, (3) Souchu et al. (2010), (4) Garrido et al. (2016), (5) AERMC (2021), (6) Ligorini et al. (2022a), and (7) Ligorini et al. (2022b).

General features (1,3,4,5,6)	Lagoon	Biguglia	Diana	Urbino	Palo
	Label of stations	BIN and BIS	DIA	URB	PAL
	Coordinates	42°36′N, 09°29′E	42°07′ N, 09°31′E	42°02′ N, 09°28′ E	41°57′N, 09°24′E
	Max depth (m)	1.8	11	9	1
	Volume (10^6 m3)	18	30	33	0.9
	Surface (km^2)	13.62	5.70	7.90	1.10
	Watershed area (km^2)	175	62	31	31
	Summer chlorophyll *a* (μg L^{-1})	14 (0.8–329)	2.0 (0.4–7.4)	1.8 (0.4–6.3)	11.7 (0.4–258)
	Summer trophic status	Eu-hypertrophic	Oligotrophic	Oligotrophic	Eu-hypertrophic
	Haline type	Meso-polyhaline	Eu-hyperhaline	Eu-hyperhaline	Poly-hyperhaline
	Annual salinity (PSU) (2023/2024)	15 (4–24)	39 (38–40)	40 (35–43)	31 (17–52)
	Annual water temperature (°C) (2023/2024)	20 (7–31)	21 (13−31)	21 (9–32)	23 (9–32)
Hydrology (2,4,6)	Connectivity to the sea	Temporary	Permanent	Temporary	Temporary
	Permanence of watercourses	Permanent	Temporary	Temporary	Temporary
Human activities (2,5,6,7)	Anthropic influence on the basin	Provision of drinking water; active fishing	Shellfish (oysters, mussels) and fish farming; active fishing	Fish farming from 1990 to 2000; active fishing	Active fishing
	Anthropic influence on the watershed	Densely populated urban area and industrial zones	Agriculture (about 10 %), mainly vineyards	Agriculture (about 45 %), mainly vineyards	Air base and commercial area

Palo (42°03′93″ N, 9°42′51″ E; named South cell) (Fig. 1). For each climatic cell, daily data were extracted from 2007 to 2023, including mean, minimum and maximum air temperature (TM, TN, TX, °C), visible radiation (SSI, W m^{-2}), cumulative rainfall (RR, mm), and mean wind speed (FFM, m s^{-1}). To reduce multicollinearity and autocorrelation, Spearman's rank correlation coefficients (ρ) were computed among variables. Based on these results (Fig. S1), only three variables, TM, RR and FFM, were retained for statistical analysis. For each climatic cell (North and South), monthly averages for temperature and wind speed, and monthly totals for rainfall were calculated, focusing on the summer period (June to August).

2.2.3. Phytoplanktonic data

Surface water samples (0–1 m) were collected in 2 L polypropylene bottles and used to quantify all phytoplankton parameters (chlorophyll *a*, abundances, and pigment diversity). For chlorophyll *a* concentration (CHLA, μg L^{-1}), 100–1000 mL, depending on site characteristics and sample concentration, were filtered under vacuum (<10 cm Hg) on Whatman GF/F membranes (25 mm diameter and 0.7 μm porosity), stored at −20 °C in glass tubes prior analysis. Samples were then ground in acetone (90 %), extracted for 24 h in the dark at 4 °C, and quantified by spectrofluorimetry with a Perkin-Elmer LS50 B. For cell abundances, 1 mL subsamples were fixed with 2 % formaldehyde (final concentration), stored in liquid nitrogen, and later analyzed by flow cytometry with a FACSCalibur flow cytometer (Becton Dickinson) following the protocols of Bec et al. (2011) and Le Ray et al. (2023). Cell counts are distinguished across three size classes: autotrophic nanophytoplankton (NANO, >3 μm), autotrophic picoeukaryotes (PEUK, <3 μm), and picocyanobacteria (<2 μm). Within the picocyanobacterial group, two subgroups are discerned: phycoerythrin-rich (PECYAN) and phycocyanin-rich (PCCYAN) picocyanobacteria. For pigment analysis, triplicate water samples (150–2000 mL, depending on biomass densities) were filtered on Whatman GF/F membranes (47 mm diameter and 0.7 μm porosity) and stored at −80 °C before analysis, and extracted during 1 h with 5 mL of a mix of acetone/methanol/water. Accessory pigment concentrations (μg L^{-1}) were measured using high-performance liquid chromatography (HPLC), allowing chemotaxonomic identification of major algal groups through pigment markers (Wright et al., 1991). This method detects pigments from microphytoplankton (>20 μm), nanophytoplankton (>3 μm), and picophytoplankton (<3 μm) size classes. 14 pigments dominant in phytoplankton groups were used as biomarkers of these groups: fucoxanthin (FUCO) and diadinoxanthin (DIAD) for diatoms, peridinin (PERI) for dinophytes, chlorophyllc2 (CHLC2) and chlorophyllc3 (CHLC3) for golden-brown algae, alloxanthin (ALLO) for cryptophytes, 19′-hexanoyloxyfucoxanthin (HEXFUCO) and 19′-butanoyloxyfucoxanthin (BUTFUCO) for haptophytes; chlorophyll *b* (CHLB), lutein (LUT), violaxanthin (VIOLA), neoxanthin (NEOX), and zeaxanthin (ZEAX) for green algae (mainly represented by chlorophytes and prasinophytes). ZEAX is also present in picocyanobacteria. Prasinoxanthin (PRASI) is a biomarker for prasinophytes (Wright et al., 1991; Roy et al., 2011; Leruste et al., 2016). To ensure data consistency following a machine upgrade in 2022, HPLC pigment data were standardized using conversion coefficients on past slopes (Mark Jr and J.W, 2015). Based on pigment concentrations, the relative proportions (%) of each pigment were calculated. The total diagnostic pigment (DP) was defined as the sum of seven pigments: FUCO, PERI, ALLO, HEXFUCO, BUTFUCO, ZEAX, and CHLB. These seven diagnostic pigments were then used to estimate the contributions of two size-class ratios: MR, representing the relative contribution of microphytoplankton compared to nano- and picophytoplankton; and NPR, expressing the combined contribution of nano- and picophytoplankton relative to microphytoplankton. These indices were adapted to our study sites from existing ratios (Roy et al., 2011; Yang et al., 2024) and calculated as follows:

$$\mathrm{MR}\ (\%) = (\mathrm{FUCO} + \mathrm{PERI})/\mathrm{DP}^{*}\ 100$$

$$\mathrm{NPR}\ (\%) = (\mathrm{ALLO} + \mathrm{HEXFUCO} + \mathrm{BUTFUCO} + \mathrm{CHLB} + \mathrm{ZEAX})/\mathrm{DP}^{*}\ 100.$$

2.3. Statistical analyses

All analyses were performed using R software (R Core Team, 2024). Climatic and physicochemical variables were ln-transformed to normalize and homogenize variances, and phytoplanktonic variables were ln(x + 1) to manage missing values and to reduce the effect of dominant groups. Because normality and homoscedasticity were not fulfilled, only non-parametric tests were conducted.

2.3.1. To identify trajectories and understand contrasted lagoon station characteristics

To identify monotonic trends on phytoplanktonic and environmental

parameters at each lagoon station (BIN, BIS, DIA, URB, PAL), Mann-Kendall tests (MK) were performed using the mk.test function from the *trend* package, which accounts for serial correlation (Pohlert, 2023). For phytoplankton and physicochemical parameters collected in the lagoons, summer averages were calculated per lagoon station. For climatic variables, summer averages of air temperature (TM) and wind speed (FFM), and summer cumulative rainfall (RR) were derived from the closest climatic cell (North cell for BIN and BIS, and South cell for DIA, URB, and PAL). All analyses covered the period 2007–2023. When one monthly value was missing, the corresponding summer value was excluded to ensure data comparability. For significant MK tests (p-value <0.05), Theil-Sen slopes and Kendall's tau coefficients were computed (Sen, 1968).

Principal Component Analyses (PCA) was conducted using the ade4 package (Dray et al., 2002) to: (i) explore relationships between phytoplankton chlorophyll *a*, abundances and pigment size-class ratios (CHLA, NANO, PEUK, PECYAN, PCCYAN, MR, NPR), physicochemical variables (TEMP, SALI, DIN, DIP, NT, PT), and climatic variables (TM, FFM, RR) across all stations, (ii) assess the main environmental and phytoplankton gradients structuring variability among stations, (iii) discriminate groups of stations for further analyses. The PCA was based on the same summer values as the ones used for MK tests.

2.3.2. To identify the relative influence of climatic and environmental drivers

To assess the relative influence of climatic drivers on phytoplankton dynamics, Generalized Additive Mixed Models (GAMMs) and Redundancy Analyses (RDA) were applied at the station group level (BIN/BIS, DIA/URB, PAL). GAMMs were used to evaluate both linear and nonlinear effects of six selected environmental variables (DIN, DIP, SALI, TM, RR, and FFM) on phytoplankton chlorophyll *a* and abundances (CHLA, NANO, PEUK, PECYAN, and PCCYAN) and the three-pigment ratio (MR, NPR). PCCYAN was modelled only for the BIN/BIS group, as it was detected in less than 15 % of samples in DIA, URB, and PAL. Conversely, PECYAN was modelled only for the DIA/URB group, since it was detected in less than 15 % of samples in BIN and BIS and occurred at very low abundances in PAL. GAMM analyses were performed with the gamm4 package (Wood and Scheipl, 2025). Random effect for Month factor (+ (1 | Month)) was applied to account for intra-summer variability. This adjustment was necessary to avoid overestimating certain effects of variables, such as the apparent relationship between high temperatures, low rainfall, and elevated Chlorophyll *a* levels, which may simply result from their simultaneous occurrence in late summer (Zhang et al., 2018). Model selection was based on the lowest Akaike Information Criterion (AIC). In parallel, Redundancy Analyses (RDA) were conducted to identify drivers of pigment contents, using pigment concentrations as response variables and the same explanatory variables as in GAMMs as predictors. The Month factor was included as a conditioning variable to account for intra-summer variability. GAMMs and RDA were complementary: GAMMs focused on integrative phytoplankton indicators (chlorophyll *a*, abundances, pigment ratios) to capture both linear and nonlinear effects of environmental drivers, while RDA was applied to analyze the linear relationships between pigment community composition and abiotic drivers.

Both GAMMs and RDA analyses were performed using phytoplankton and physicochemical raw data collected monthly in the lagoons, instead of using summer averages derived from three values. To associate exact climatic conditions, daily climatic data were extracted from the SAFRAN system for the 30 days preceding each sampling event instead of relying on fixed monthly values, thus accounting for variability in sampling dates across years and stations. Values were computed for each lagoon station based on its corresponding climatic cell (North or South), allowing precise alignment between each sample and preceding weather conditions. To refine the detection of climatic effects on phytoplankton dynamics, a sliding window analysis was applied using the *climwin* package adapted to our dataset (Bailey and Pol, 2016) to identify the most relevant temporal window to calculate climatic sums and averages. To capture short-term climate influences accounting for the rapid turnover of phytoplankton communities, we tested time windows ranging from 1 to 15 days before each sampling. Linear models were fitted for each phytoplankton parameter (CHLA, abundances, and pigment ratios), with the three combined climatic variables (TM, RR, FFM). Model performance was evaluated using AIC, and the optimal time window, minimizing the average AIC across all models, was identified as the 7 days preceding sampling. This 7-day window was subsequently used to calculate cumulative rainfall, mean air temperature, and wind speed, and these values were then associated with the corresponding monthly lagoon data.

Due to strong correlations between CHLA and total nitrogen and phosphorus concentrations (NT, PT), as these variables include the particulate organic fraction directly linked to phytoplankton biomass (Souchu et al., 2010), NT and PT were excluded from the GAMMs and RDA models. Only inorganic nutrient forms (DIN, DIP) were retained to characterize nutrient control.

3. Results

3.1. Long-term dynamics and trajectories

Summer values of phytoplankton chlorophyll *a* (CHLA) and abundances (NANO, PEUK, PCCYAN, PECYAN) revealed strong differences between lagoon stations (Fig. 2). CHLA reached higher monthly maxima at BIS, BIN, and PAL, with values up to 216 and 329 μg L^{-1} in 2007, respectively at BIS and BIN, and up to 258 μg L^{-1} in 2010 at PAL. For DIA and URB, monthly values remained consistently low (below 8 and 7 μg L^{-1} respectively). Clear distinctions were also observed in picocyanobacterial composition between stations: PCCYAN consistently dominated in BIN and BIS (respectively up to 9432 and 6977 $\times$ 10^6 cells L^{-1} in 2007), were nearly absent in DIA and URB (respectively below 16 and 46 $\times$ 10^6 cells L^{-1}), and appeared as anecdotal peaks in PAL (up to 6203 $\times$ 10^6 cells L^{-1} in 2010). Inversely, PECYAN consistently dominated in DIA and URB (reaching monthly maxima 657 and 1192 $\times$ 10^6 cells L^{-1}, respectively), were nearly absent in BIN and BIS (respectively below 6 and 0.3 $\times$ 10^6 cells L^{-1}), and occurred frequently but at low levels in PAL (below 36 $\times$ 10^6 cells L^{-1}; Fig. 2 and Fig. S2).

In addition to station-specific differences, pronounced interannual variability was observed within stations. Mann-Kendall trend tests performed on summer means revealed significant monotonic trends for some parameters and stations (Table 2). At the BIN station, PEUK abundance declined significantly ($p = 0.022$), while at the BIS station, significant decreases were observed for CHLA, NANO, PEUK, and PCCYAN ($p = 0.03$, 0.019, 0.001, and 0.007, respectively), reflecting contrasted trajectories within the same lagoon. A decreasing trend was also detected for CHLA at the URB station ($p = 0.009$).

Pigment data were used to characterize taxonomic composition and compute pigment ratios to evaluate the relative contribution of microphytoplankton (MR) compared to nano-picophytoplankton (NPR) size classes (Fig. S2). The summer mean relative contributions and dominance of pigment ratios varied across stations and years (Fig. 3). MR frequently dominated at all stations with a minimum of 18 % in 2009 at BIS (37 % of alloxanthin contribution). MR contributions peaked at 93 % at DIA in 2009 (including 53 % fucoxanthin), and also reached high values in 2016 at BIS (90 %, including 44 % peridinin), URB (85 %, including 29 % fucoxanthin and 23 % peridinin), and PAL (90 %, including 41 % fucoxanthin). NPR rarely exceeded MR at DIA, URB, or PAL, except in 2018 at DIA and PAL where it reached 60 %, and at URB in 2021 where it reached 57 % (including 45 % chlorophyll *b*). At BIN and BIS, NPR exceeded MR for several years. However, NPR ratios have higher sustained values since 2020 at URB and PAL, rising from a mean of 31 % before 2020 to 52 % afterwards at URB and from 27 % to 42 % at PAL. At the pigment level within the microphytoplankton size class,

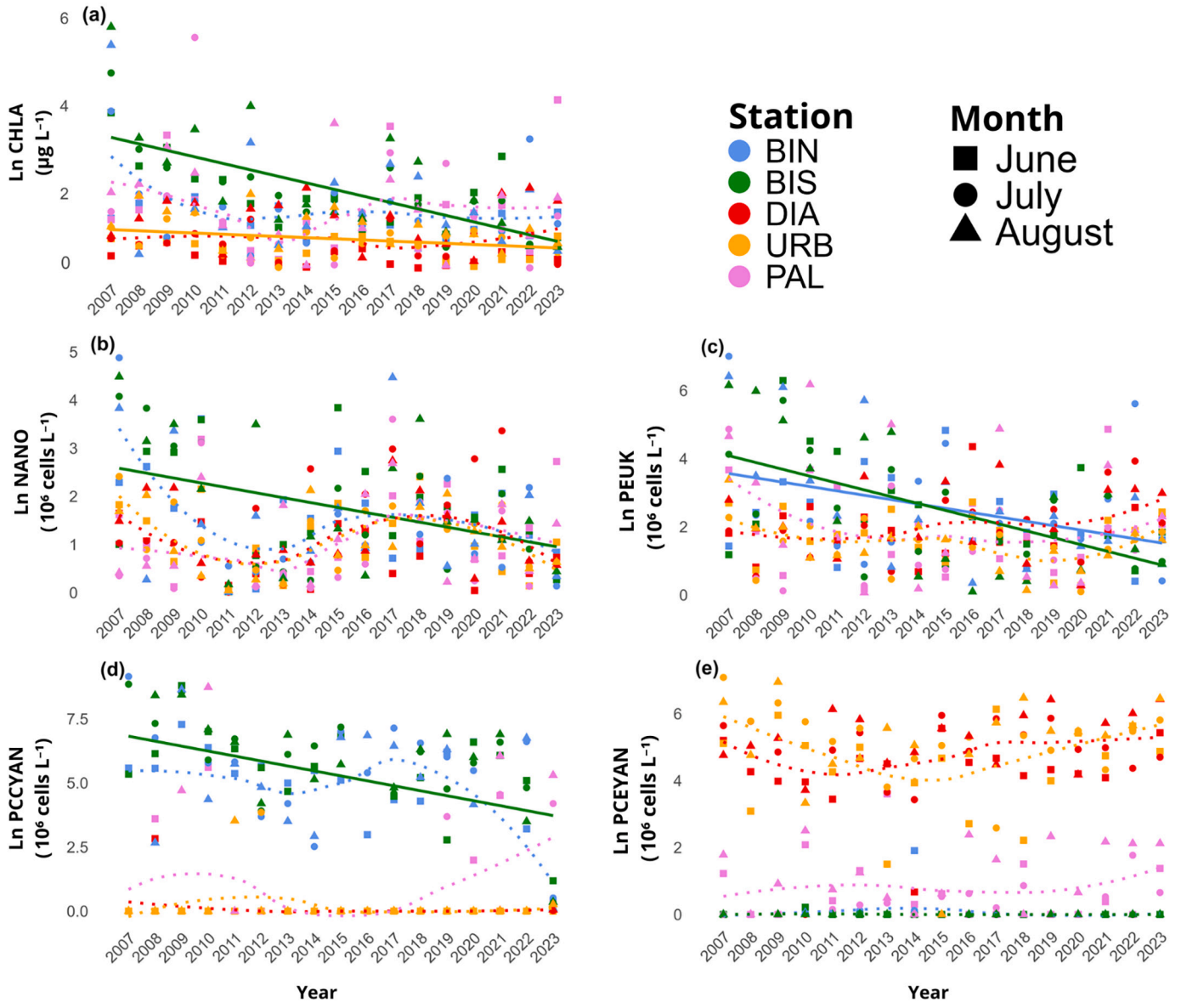

Fig. 2. Time series of five phytoplankton variables: (a) CHLA, (b) NANO, (c) PEUK, (d) PCCYAN and (e) PECYAN; at each station (BIN, BIS, PAL, DIA, URB), based on summer data (June to August). A solid Linear curve indicates a significant trend as detected by the Mann–Kendall test, while a dashed LOESS curve denotes a non-significant trend. Monthly data points are displayed using symbols: squares for June, circles for July, and triangles for August. All data were ln-transformed.

fucoxanthin consistently dominated in DIA and URB, with summer mean contributions always reaching up to 23 %. In contrast, BIN, BIS, and PAL exhibited alternating dominance between fucoxanthin and peridinin (Fig. 3). MK trend tests on pigment summer data revealed significant trajectories. At BIS, several significant pigment trends were observed, with a decline in fucoxanthin ($p = 0.026$), zeaxanthin ($p < 0.015$) and lutein ($p = 0.002$), and an increase in peridinin ($p = 0.02$). In contrast at BIN, only a decrease in fucoxanthin was detected ($p = 0.015$). These trends suggest a progressive shift in dominance from diatom to dinoflagellate taxa, along with a decline in picophytoplankton groups such as picocyanobacteria and/or chlorophytes (Table 2). Chlorophyll b monotonically increased at three stations, PAL ($p = 0.002$), DIA ($p = 0.013$), and URB ($p = 0.014$), suggesting a rise in chlorophytes. Additionally at PAL, a monotonic increase in prasinoxanthin ($p = 0.035$) and a monotonic decrease in diadinoxanthin ($p = 0.009$; Table 2) were observed. In addition, at DIA, chlorophyll *c*3 monotonically decreased ($p = 0.028$), while at URB, neoxanthin monotonically decreased ($p < 0.0005$) and was not detected after 2018 (Fig. 3; Fig. S2).

Clear differences between stations were also observed on physico-chemical variables (Fig. S3). Monthly concentrations of total nitrogen (NT) reached up to 472 and 427 µmol L^{-1}, respectively, at BIN and BIS in 2007, and up 119 µmol L^{-1} in 2010 at PAL, while maximum values remained much lower at DIA (47 µmol L^{-1} in 2015) and URB (29 µmol L^{-1} in 2020). Monthly concentrations for dissolved inorganic nitrogen (DIN) reached up to 18, 27, and 24 µmol L^{-1}, respectively, at BIN, BIS, and PAL, while they remained below 3.8 and 4.2 µmol L^{-1}, respectively, at DIA and URB. Salinity also differed between stations: BIN and BIS were characterized by lower but variable salinities, with BIN being saltier than BIS (monthly values respectively between 7–34 and 4–28 PSU). In contrast, DIA and URB had higher salinities, more stable at DIA (respectively between 36–41 and 32–43 PSU). PAL, which exhibited more variable salinities, occasionally reaching very high levels (23–47 PSU). Beyond these differences, the MK trend tests on summer means revealed contrasting trajectories. At BIN, DIP concentrations monotonically increased ($p = 0.000$), while they decreased at DIA ($p = 0.023$). At URB, Total phosphorus (PT) concentrations monotonically decreased

Table 2
Results of significant Mann-Kendall (MK) trend tests performed on summer means for phytoplankton and physicochemical variables by stations (BIN, BIS, DIA, URB, PAL). For climatic variables, trend tests were performed on summer means for air temperature and wind speed and on summer totals for rainfall, by climatic cell (North and South). Only significant results are shown in the table (*** $p < 0.001$; ** $p < 0.01$; * $p < 0.05$). Statistically significant *p*-values are highlighted in bold, and the table includes Kendall's Tau, Sen's slope and the direction of the trend (indicated by green and red arrows).

Station	Parameter	*P* value	Tau	Sen Slope	Trend
BIN	PEUK	0.022*	−0.433	−0.110	↘
	FUCO	0.015*	−0.441	−1.384	↘
	DIP	0.000***	0.767	0.139	↗
BIS	CHLA	0.003**	−0.544	−0.144	↘
	PEUK	0.001**	−0.618	−0.263	↘
	NANO	0.001**	−0.618	−0.263	↘
	PCCYAN	0.019*	−0.426	−0.150	↘
	PERI	0.021*	0.421	1.405	↗
	FUCO	0.026*	−0.406	−1.777	↘
	ZEAX	0.015*	−0.441	−1.090	↘
	LUT	0.002**	−0.554	−0.186	↘
DIA	CHLB	0.013*	0.450	0.448	↗
	CHLC3	0.028*	−0.403	−0.298	↘
	DIP	0.023*	0.404	0.36	↘
URB	CHLA	0.009**	−0.471	−0.036	↘
	CHLB	0.014*	0.451	0.382	↗
	NEOX	0.000***	−0.760	−0.124	↘
	SALI	0.009**	0.471	0.006	↗
	PT	0.047*	−0.377	−0.025	↘
PAL	CHLB	0.002**	0.557	0.965	↗
	DIAD	0.009**	−0.471	−0.322	↘
	PRASI	0.035*	0.398	0.232	↗
	TEMP	0.036*	0.382	0.007	↗
North climatic cell	FFM	0.023*	0.412	0.006	↗
South climatic cell	TM	0.029*	0.397	0.004	↗

($p = 0.047$), and a significant monotonic increase in salinity was detected ($p = 0.009$) (Table 2). At PAL, a significant monotonic increase in water temperature (TEMP) was detected ($p = 0.036$), with high amplitude of values (19–33 °C). No significant temporal trends were detected for total nitrogen (NT) and DIN across the five stations, but DIN peaks at BIS appeared less frequent during July and August in recent years (Fig. S2). For climatic variables, mean summer air temperature (TM) significantly increased at the South climatic cell (+ 0.1 °C /year, $p = 0.029$), while mean summer wind speed (FFM) increased at the North climatic cell (+0.008 m s^{-1} /year, $p = 0.023$). Summer 2022 was the warmest on record, with mean summer air temperature reaching 25.9 °C in the South cell and 25.5 °C in the North cell. Summer 2012 was the driest, with summer cumulative rainfall as low as 7.2 mm in the South cell and 4.7 mm in the North cell (Fig. S3).

3.2. Phytoplankton community composition conditioned by physicochemical contrasts across lagoon stations

The contrasts in phytoplankton, physicochemical, and climatic patterns between stations led us to investigate which factors best explain these observed differences and allow for a clearer distinction, while assessing temporal variability. A Principal Component Analysis (PCA) was performed on summer means per station, based on phytoplankton chlorophyll *a*, abundances and pigment ratios, physicochemical and climatic variables. This PCA (Fig. 4a) indicates that nutrient concentrations and salinity were the primary drivers of phytoplankton community structure, while variability in phytoplankton composition and physicochemical conditions was poorly associated with climatic variability. The first axis (PC1), which explained 36.7 % of the total variance, highlighted strong contrasts among stations, along a gradient driven in negative by total and inorganic nutrient concentrations (NT, PT, DIN, DIP), chlorophyll *a* (CHLA), and the abundances of phycocyanin-rich picocyanobacteria (PCCYAN), picoeukaryotes (PEUK), and nanophytoplankton (NANO); and in positive by salinity (SALI) and phycoerythrin-rich picocyanobacteria (PECYAN). This gradient separated the stations into three groups (Fig. 4b). BIN and BIS were located on the negative side of PC1 (with BIS showing greater variability), characterized by higher nutrient levels, lower salinities, and a strong dominance of PCCYAN (Fig. 2). DIA and URB were located on the positive side of PC1, characterized by lower nutrient levels, higher and stable salinities, and a strong dominance of PECYAN. PAL occupied an intermediate position, marked by variable trophic levels and salinity, including occasional peaks of very high salinity, and by no dominance of a picocyanobacterial group. BIS and PAL display the largest ellipses, indicating strong temporal fluctuations, while BIN, DIA, and URB showed more stable profiles. These patterns enabled the aggregation of stations into three distinct groups: BIN/BIS as meso-polyhaline and eu-hypertrophic stations dominated by PCCYAN; DIA/URB as eu-hyperhaline and oligotrophic stations dominated by PECYAN; and PAL as a poly-hyperhaline, eu-hypertrophic station without picocyanobacterial dominance.

The second axis (PC2) explained 17.3 % of the total variance and primarily reflected a climatic gradient, positively driven by air temperature (TM) and water temperature (TEMP), and negatively by rainfall (RR) and wind (FFM). PAL exhibited higher mean water temperature values (Fig. S3). Pigment ratios were more influenced by this climatic gradient than by physicochemical conditions (Fig. 4a), with the micro-phytoplankton ratio (MR) being associated with TM, while the nano-picophytoplankton ratio (NPR) was associated with RR. No temporal pattern related to the distribution of years was detected (Fig. S4).

3.3. Abiotic drivers of phytoplankton dynamics

To identify the main abiotic drivers of phytoplankton dynamics, we combined two complementary approaches to assess the relative influence of six selected variables on phytoplankton dynamics: three climatic metrics (mean air temperature, wind speed, and rainfall); inorganic nutrient concentrations (DIN and DIP), and salinity (SALI). Models were fitted separately for each group of stations (BIN/BIS, DIA/URB, PAL). Generalized Additive Mixed Models (GAMMs) were used to explore both linear and nonlinear effects of environmental variables on seven phytoplankton parameters, including phytoplankton biomass and

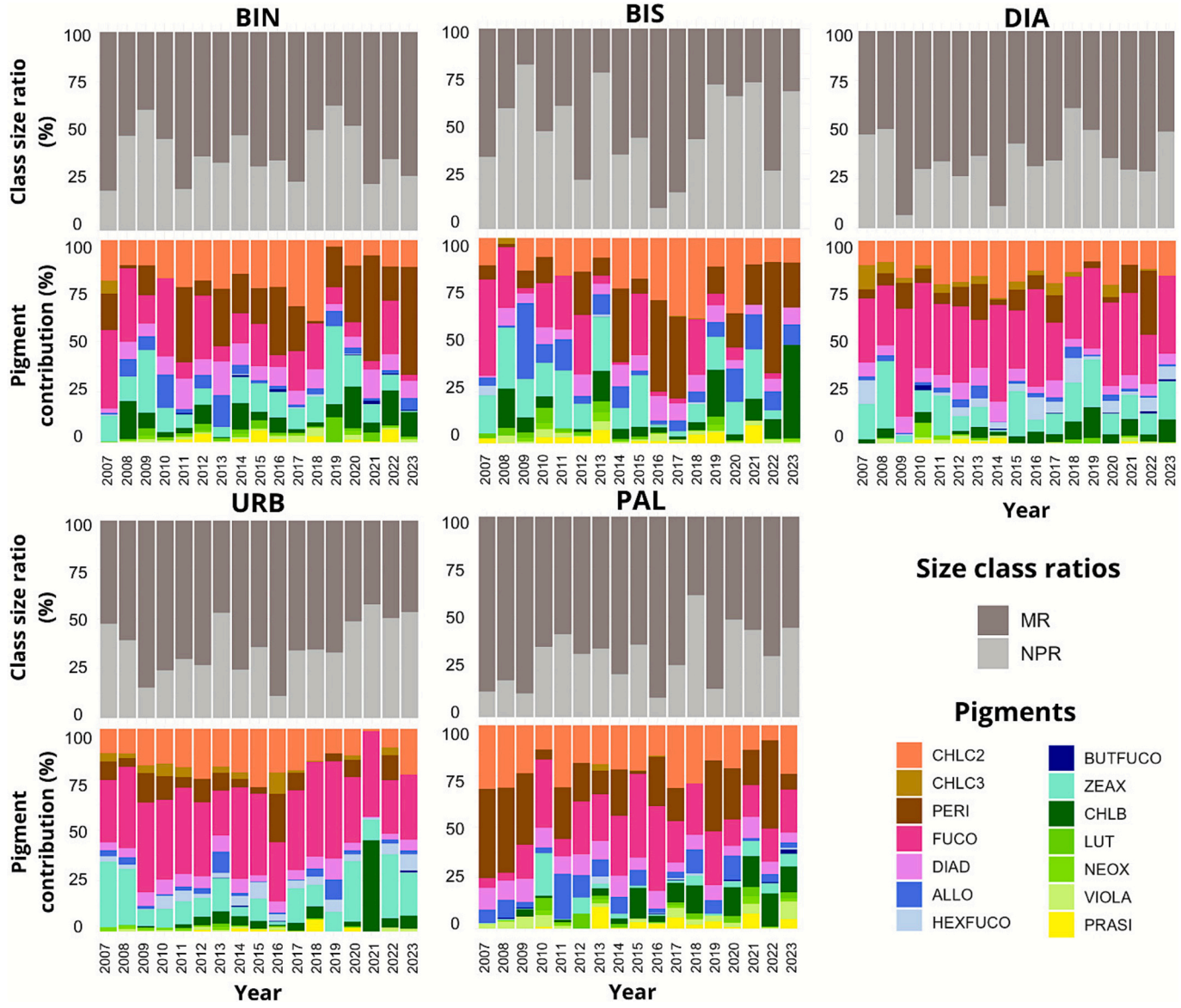

Fig. 3. Summer mean proportions of 14 accessory pigments and two pigment size-class ratios (MR: microphytoplankton, NPR: nano-picophytoplankton) at the five stations (BIN, BIS, DIA, URB, PAL) from 2007 to 2023. The upper panels show the relative contributions of the two ratios, while the lower panels illustrate the annual composition of accessory pigments, expressed as percentages of total accessory pigment biomass.

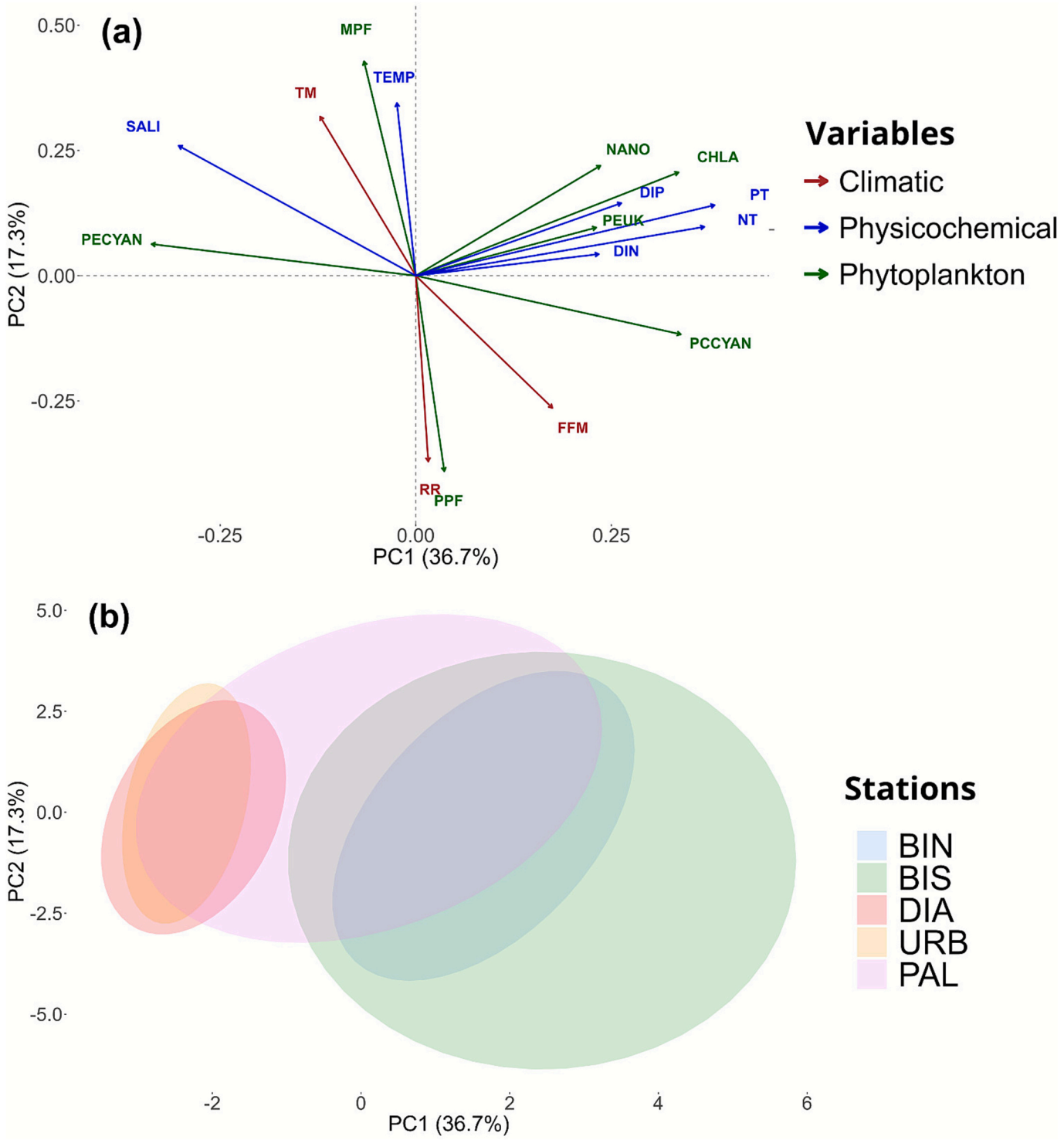

Fig. 4. Principal Component Analysis (PCA) performed on seven phytoplankton variables (green vectors; CHLA, NANO, PEUK, PCCYAN, PECYAN, MR, NPR) and nine environmental variables, including climatic (browns vectors; TM, RR, FFM) and physicochemical (blue vectors; DIN, DIP, NT, PT, SALI, TEMP) parameters, using summer means data from five stations (BIN, BIS, DIA, PAL, URB), over 17 years of sampling (2007–2023). (a) Correlation circle showing the contribution of variables to the first two principal components (PC1: 36.7 %, PC2: 17.3 %). (b) Ordination of samples grouped by station typology, with 95 % confidence ellipses. (For interpretation of the references to colour in this figure legend, the reader is referred to the web version of this article.)

Table 3
Summary of Generalized Additive Mixed Models (GAMMs) linking seven phytoplankton variables (CHLA, NANO, PEUK, PCCYAN, PECYAN, MR, NPR) to nutrients (DIN, DIP), salinity (SALI), and climatic drivers (TM: air temperature, RR: precipitation, FFM: wind). Models were performed separately for each phytoplankton variable within each station group (BIN/BIS, DIA/URB, and PAL), and the best model was selected based on the Akaike Information Criterion (AIC). For each explanatory variable, estimates are reported for linear effects, and estimated degrees of freedom (EDF) for nonlinear effects (edf > 2), with significance levels indicated (*** $p < 0.001$; ** $p < 0.01$; * $p < 0.05$), effects are color-coded to indicate their nature and direction: green for significant positive linear effects, red for significant negative linear effects, and blue for significant nonlinear effects. Model performance is indicated by the AIC value and the percentage of deviance explained.

Station groups	Response's variables	DIN	DIP	SALI	TM	RR	FFM	Explained deviance	AIC	Month effect	Intercept
BIN/BIS	CHLA	4.42 ***		-0.42 *	2.72 **			47%	221		***
	NANO	3.40 ***			4.42 **			30%	271	*	*
	PEUK	2.61 ***						26%	329		***
	PCCYAN			2.69 *				11%	417		***
	MR	3.36 *	5.32 *					35%	232		
	NPR	2.69 *		-0.43 *				18%	250		***
DIA/URB	CHLA		0.15 **				0.82 **	46%	100	***	**
	NANO		0.27 **		3.13 *	0.24 **		23%	207	*	*
	PEUK			3.86 **		0.19 *		23%	309		***
	PECYAN				3.20 *			5%	318		
	MR										
	NPR										
PAL	CHLA		3.26 ***	2.48 *		0.20 *		72%	78		***
	NANO		0.36 **					15%	120		***
	PEUK	0.75 ***						25%	162		***
	MR				2.63 **	0.23 *		20%	63		
	NPR		2.85 *		-6.77 ***	-0.46 **		47%	119		***

abundances (CHLA, NANO, PEUK, PCCYAN, PECYAN) and pigment ratios (MPR, NPR). The best models were selected based on the lowest AIC (Table 3). In parallel, to explore how the phytoplankton pigment contents responded to abiotic conditions, a Redundancy Analysis (RDA) was conducted to assess the relationships between environmental gradients and the composition of the pigment community, based on the concentrations of fourteen pigments.

In the BIN/BIS group, phytoplankton variables were mainly influenced by inorganic nutrient concentrations. For CHLA, the outputs of the GAMM model revealed a nonlinear exponential effect of DIN ($p < 0.001$), a positive linear effect of TM ($p < 0.01$), and a negative effect of SALI ($p < 0.05$) (Table 3). Similar nonlinear exponential effects of DIN were observed for both NANO ($p < 0.001$) and PEUK ($p < 0.001$) abundances, with an additional positive effect of TM ($p < 0.01$) and a significant Month random effect for NANO ($p < 0.05$). The PCCYAN model, only fitted for BIN/BIS, showed a nonlinear U-shaped effect of SALI ($p < 0.05$). Pigment ratios showed a nonlinear exponential effect of DIN ($p < 0.05$) and a nonlinear U-shaped effect of DIP ($p < 0.05$) on MR, and a nonlinear decreasing effect of DIN ($p < 0.05$) and a negative effect of SALI ($p < 0.05$) on NPR. The RDA conducted for BIN/BIS (Fig. 5a) was significant ($F = 1.92$, $p = 0.007$), with DIN, DIP, and TM highlighted as significant predictors of phytoplankton variables (p values respectively 0.019, 0.022, 0.027). The first axis (RDA1), which explained only 6 % of the total variance, as most of the pigments remained close to the barycenter, was structured by a contrast between DIN and DIP concentrations. FUCO was positively associated with DIN, while PERI was associated with DIP and salinity. The second axis (RDA2) explained only 3 % of the variance, with an opposition between RR and TM associated with FUCO.

In the DIA/URB group, stronger and more visible climatic signals were observed on phytoplankton variables, which can even exceed the influence of nutrient concentrations. For CHLA, the GAMM model showed linear positive effects of both FFM ($p < 0.01$) and DIP ($p < 0.01$) with a significant Month random effect ($p < 0.001$). For NANO, DIP had a positive effect ($p < 0.01$), along with positive effects of TM ($p < 0.05$) and RR ($p < 0.01$). PEUK showed a nonlinear effect of SALI ($p < 0.01$) characterized by an increase beyond a high salinity threshold, and a linear positive effect of RR ($p < 0.05$). The PECYAN model, only applied to DIA/URB, showed a unique linear positive effect of TM ($p < 0.05$). For pigment ratios, no significant effects of environmental variables were detected (Table 3). The RDA for DIA/URB (Fig. 5b) was significant ($F = 2.10$, $p = 0.02$), with significant effects of RR and FFM (p values respectively 0.004 and 0.041). The first axis (RDA1) explained 10 % of the total variance and was structured by FFM, RR, and DIP. FUCO, CHLC2, and PERI were positively associated with all three variables, and especially with FFM, similar to what was observed for the GAMM built for CHLA in this group. The second axis (RDA2) explained only 1 % of the variance, with a slight opposition between SALI and DIN.

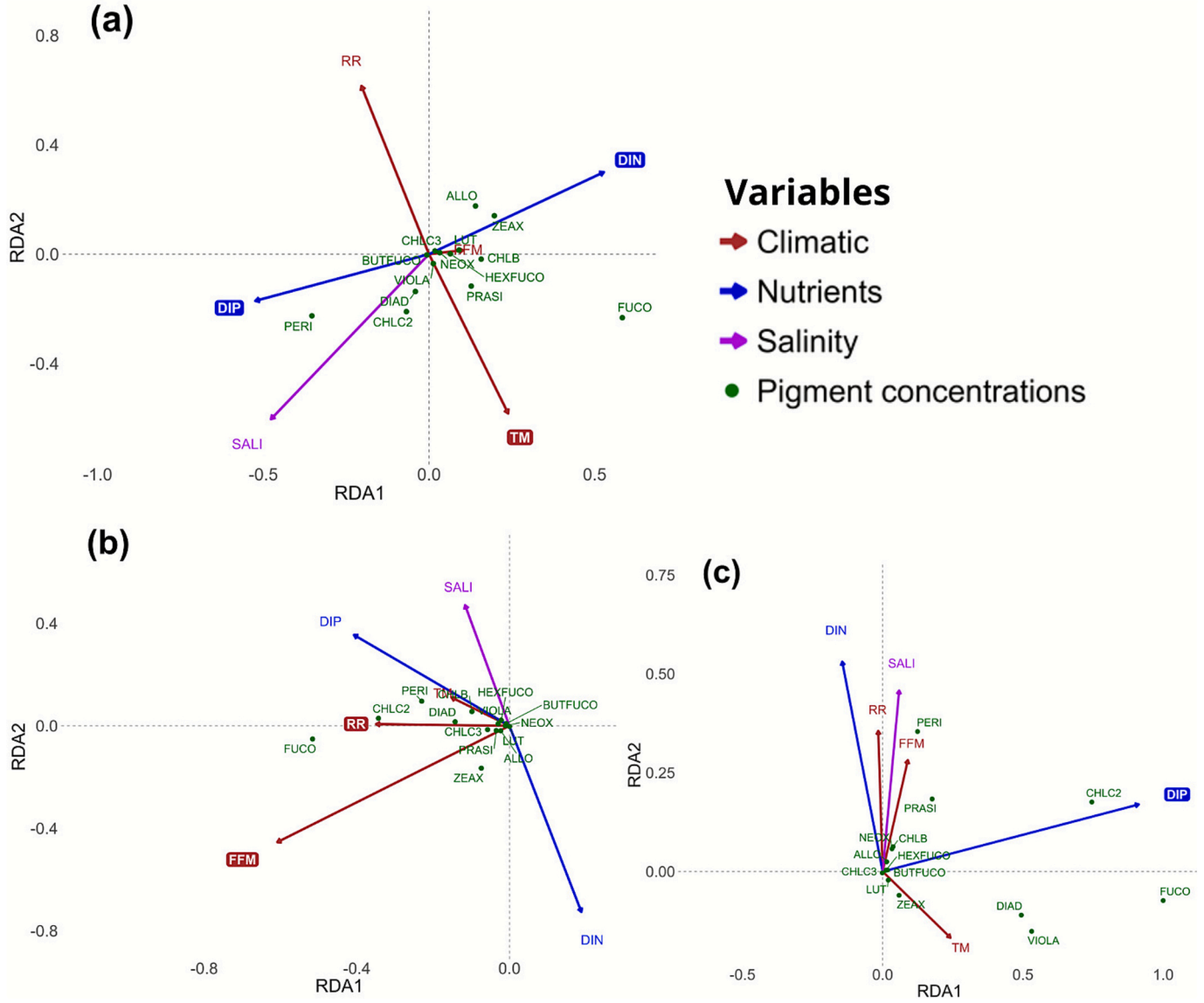

Fig. 5. Redundancy Analysis (RDA) biplots illustrating the relationships between phytoplankton pigment concentrations and environmental variables for each lagoon group: (a; BIN/BIS), (b; DIA/URB), and (c; PAL). Arrows represent six environmental variables: air temperature (TM), precipitation (RR), wind speed (FFM), dissolved inorganic nitrogen (DIN), dissolved inorganic phosphorus (DIP), and salinity (SALI). Explanatory variables with significant effects are highlighted. Green points correspond to the 14 accessory pigments used as phytoplankton functional markers: fucoxanthin (FUCO), peridinin (PERI), alloxanthin (ALLO), chlorophyll *b* (CHLB), zeaxanthin (ZEAX), lutein (LUT), neoxanthin (NEOX), violaxanthin (VIOLA), prasinoxanthin (PRASI), 19′-hexanoyloxyfucoxanthin (HEXFUCO), 19′-butanoyloxyfucoxanthin (BUTFUCO), diadinoxanthin (DIAD), chlorophyll *c*2 (CHLC2), and chlorophyll *c*3 (CHLC3). (For interpretation of the references to colour in this figure legend, the reader is referred to the web version of this article.)

In the PAL group, phytoplankton variables were more influenced by nutrient concentrations than in DIA/URB, but less than in BIN/BIS, and involved different nutrient sources. The GAMM model for CHLA showed a nonlinear exponential effect of DIP ($p < 0.001$), a nonlinear U-shaped effect of SALI ($p < 0.01$), and a positive linear effect of RR ($p < 0.05$). For NANO, a unique positive linear effect of DIP ($p < 0.01$), and for PEUK, a unique positive linear effect of DIN ($p < 0.001$) were observed (Table 3). For pigment ratios, MR was positively affected by TM ($p < 0.01$) and RR ($p < 0.05$), while NPR was negatively impacted by TM and RR ($p < 0.0001$ and $p < 0.01$) and a nonlinear decreasing effect of DIP ($p < 0.05$). The RDA model for PAL (Fig. 5c) was also significant ($F = 2.74$, $p = 0.01$), with DIP as the only significant explanatory variable (p-value = 0.001). The first axis (RDA1) explained 25 % of the total variance and was structured by DIP, which was positively linked to FUCO, CHLC2, and to a lesser degree, DIAD and VIOLA. TM showed a slight positive association with DIAD and VIOLA, and was positively correlated with DIP. The second axis (RDA2) explained only 3 % of the variance, with a slightly positive association between PERI, SALI, and DIN.

4. Discussion

This study, based on long-term summer monitoring of four contrasted Mediterranean coastal lagoons, aimed to evaluate the influence of climatic and nutrient drivers on phytoplankton dynamics and explored how these communities may evolve under climate change.

4.1. Contrasted temporal trends across lagoons

Long-term monitoring highlighted different phytoplankton and environmental temporal trends across lagoons, potentially reflecting distinct functioning and evolutionary drivers. In the meso-polyhaline and eu-hypertrophic lagoon (Biguglia), pronounced contrasts also

emerged between stations. At the southern station, marked declines occurred in chlorophyll *a* biomass, nanophytoplankton, picoeukaryotes, PC-rich picocyanobacteria, and several pigments including fucoxanthin (a diatom marker), while at the northern station declines were restricted to fucoxanthin and picoeukaryotes. These differences likely reflect the stronger historical watershed influence in the south (Garrido et al., 2016), which likely increased turbidity and reduced water-column stability and light penetration, thereby influencing phytoplankton distribution. However, the observed trajectories point to a progressive oligotrophication process, potentially supported by the management plan in 2008 to reduce nutrient inputs (Ligorini et al., 2022b) and consistent with the, though nonsignificant, decline in nitrogen concentrations. This suggests that nutrient limitation acted as the main driver of phytoplankton trends, consistent with observations from other Mediterranean lagoons undergoing nutrient load reductions (Collos et al., 2009; Derolez et al., 2019; Leruste et al., 2016) and with the resource control model of Jeppesen et al. (2007). As nitrogen pressure seems to have declined, a concurrent increase in peridinin and DIP suggests higher phosphorus availability and a growing contribution of dinoflagellates, which are slow-growing and often mixotrophic (Ligorini et al., 2022a; Bi et al., 2021). Phosphorus enrichment could also be sustained by hydrological modifications (Garrido et al., 2016) and by sedimentary phosphorus release under warmer conditions (Pesce et al., 2018). Such nutrient regime shifts are known to restructure phytoplankton communities (Berger et al., 2006; Cecchi et al., 2016; Thomas et al., 2017; Ouaissa et al., 2023). Since diatoms may become more sensitive to warming under nutrient limitation (Thomas et al., 2017), this shift toward dinoflagellates could be further amplified under future climatic conditions (Bi et al., 2021). But nutrient dynamics are not necessarily the sole explanation for the biomass decline and community shifts. Hydrodynamic instability may also have influenced the observed trends through both anthropogenic and climate-related processes. Management actions, such as the operation of the Fossone Canal (Garrido et al., 2016), may have triggered turbid phases by resuspending sediments and increasing suspended matter in the surface layer of the water column (Zaldívar et al., 2008; De Oliveira et al., 2023). These conditions reduced light penetration and limited phytoplankton growth (Lopes et al., 2019), although nutrient release may have partly mitigated biomass decline (Jiang et al., 2022). By contrast, reduced nutrient inputs combined with warming-induced reductions in freshwater inflows and the altered flow regime of the Golo River may have promoted water column clarity but lower nutrient supply (Shalby et al., 2020; Sabater et al., 2023). The increasing alternation between turbid and clear phases likely further destabilized phytoplankton dynamics and contributed to phytoplankton declines. This aligns with the Margalef model, which highlights the interplay between resource availability and hydrodynamic forcing in shaping phytoplankton succession (Margalef, 1978). Salinity fluctuations in this anthropized meso-polyhaline system may have directly imposed osmotic stress on phytoplankton by altering physiological processes (D'ors et al., 2016; Ligorini et al., 2023), while also exerting indirect effects by modifying nutrient concentrations (Wang et al., 2025).

The deeper, eu-hyperhaline and oligotrophic lagoons (Diana and Urbino) maintained greater ecological and physicochemical stability over time, showing fewer linear trends. Diatom dominance persisted with a high and stable contribution of fucoxanthin across all years, although at Diana the previously reported increase in diatom abundance (Ligorini et al., 2022a) was no longer evident from fucoxanthin contribution. In Urbino, a significant salinization trend emerged, undetected in earlier studies (Ligorini et al., 2022a), suggesting warming-driven changes.

Palo, the smaller and more confined poly-hyperhaline system, appears to be the most unstable with pronounced interannual fluctuations but few linear trends. However, the significant increase in water temperature, combined with persistent hyperhalinity and a sustained contribution of nano-picophytoplankton pigment ratio in recent years, may suggest a shift toward an ecosystem structure increasingly driven by warming (Bec et al., 2011; Winder and Sommer, 2012; Valenti et al., 2016; Doré et al., 2022; Ligorini et al., 2023).

Climatic trends also highlighted contrasts in local climate dynamics. Mean summer air temperature increased significantly only in the southern climatic cell, while summer wind speed increased in the northern cell. No significant rainfall trends were detected. These findings partially align with other studies across the Mediterranean Basin, reporting rising temperatures but no consistent summer trends in wind or rainfall (Ligorini et al., 2022b; Grossi et al., 2024), whereas projections indicate a significant decrease in summer rainfall in the coming decades (Pesce et al., 2018). This also confirms that local climatic trajectories can diverge from global patterns (Guzmán et al., 2023). Nevertheless, values derived from climatic reanalysis datasets should be interpreted with caution when assessing long-term trends (Vidal et al., 2010).

In addition, trend detection remains sensitive to the temporal scale considered and may be disrupted by extreme events, which can interrupt the emergence of linear trends.

4.2. *Contrasting phytoplankton responses reveal that different abiotic drivers prevail across systems*

Our PCA analysis reveals a clear separation among lagoon stations, structured along gradients of physicochemical conditions and phytoplankton parameters. This segregation distinguishes Biguglia, Palo, and the pair of Diana and Urbino, with differences in nutrient and salinity levels, phytoplankton community composition, likely reflecting contrasting dynamics despite their spatial proximity within a Mediterranean climate. Additionally, multivariate analyses collectively revealed that the relative weight of climatic versus nutrient drivers differs between lagoon groups. This heterogeneity provides a basis for disentangling the respective roles of environmental and climatic controls in shaping site-specific phytoplankton dynamics.

GAMMs and RDA consistently indicated that in nutrient-enriched lagoons (Biguglia and Palo), inorganic nutrient concentrations were the main drivers of phytoplankton dynamics, explaining more variability than climatic factors. In Biguglia, the most anthropized system, dissolved inorganic nitrogen concentrations (DIN) promoted chlorophyll *a*, picoeukaryotes, and the microphytoplankton (MR) size class, while DIP had a positive effect on peridinin and nanophytoplankton. GAMMs on pigment ratios suggest an exclusion of smaller size classes under nutrient-rich conditions (Leruste et al., 2019). This highlights the central role of nutrient enrichment and DIN/DIP ratio in structuring phytoplankton communities in this system (Ouaissa et al., 2023). In Palo, a less anthropized but smaller and confined system, DIP emerges as the dominant driver, enhancing chlorophyll *a*, nanophytoplankton abundance, and fucoxanthin, suggesting that phosphorus enrichment supports diatom development, a competitive group favored under nutrient-rich conditions (Margalef, 1978). Episodes of synchronous peaks in nutrients and chlorophyll *a* (CHLA $>200\ \mu g\ L^{-1}$; August 2007 in Biguglia; July 2010 in Palo), with high fucoxanthin and absence of picophytoplankton pigments (zeaxanthin, chlorophyll *b*), confirm the strong nutrient control and rapid and size-selective response to enrichment (Zaldívar et al., 2008; Collos et al., 2009). These findings are consistent with broader observations that nutrient pulses favor larger, fast-growing taxa such as diatoms (Leruste et al., 2021; Ouaissa et al., 2023; To et al., 2025). Climatic signals were detectable, as air temperature increased chlorophyll *a* and nanophytoplankton in Biguglia, while rainfall enhanced chlorophyll *a* and microphytoplankton ratio in Palo, but they remained secondary and potentially confounded with nutrient effects.

By contrast, phytoplankton dynamics in nutrient-poor systems (Diana and Urbino) were more strongly shaped by climatic drivers, which explained a significant proportion of the variability in most of the phytoplankton parameters in GAMMs and RDA analyses, equaling or

exceeding the influence of inorganic nutrients. Among these drivers, air temperature (TM) strongly positively influenced nanophytoplankton abundance and was the only significant predictor of PE-rich picocyanobacteria (PECYAN) abundance. Our summer monthly data reveal a thermal threshold around 26 °C, below which PECYAN abundances consistently remained under 275×10^6 cells L^{-1}, consistent with optimal growth of warm-adapted Mediterranean *Synechococcus* thermotypes in oligotrophic systems (Doré et al., 2022). Maximal abundances above 29 °C confirm their optimal proliferation under warming (Collos et al., 2009; Derolez et al., 2020). Although not statistically significant, sustained abundances of PECYAN in recent years (Fig. S1) suggest their stable presence. PECYAN group is adapted to warm, saline, stratified, and nutrient-poor conditions (Collos et al., 2009; Bec et al., 2011; To et al., 2025), likely reflecting the indirect effects of warming, which enhances water-column stratification and reduces nutrient renewal in surface layers (Da Costa et al., 2022; Vereshchaka et al., 2023). In addition to their thermal tolerance, their physiological plasticity, low palatability, and migration capacity (Valenti et al., 2016; Grébert et al., 2018; Pomati et al., 2020) make them indicators of both warming and oligotrophication dynamics in the Mediterranean region (Bec et al., 2011).

Wind also emerged as a key driver, with strong positive effects on chlorophyll *a* and fucoxanthin concentrations (Zhang et al., 2018), suggesting that wind favors diatoms, a turbulence-tolerant taxon responsive to nutrient enrichment (Leruste et al., 2019; Sabater et al., 2023; Talavera et al., 2024). Its combined effect with DIP further indicates that wind may enhance phosphorus availability through mixing and sediment resuspension (Zaldívar et al., 2008; Winder and Sommer, 2012; Lopes et al., 2019). In low-renewal systems, it can even dominate over tidal circulation, driving water and particulate matter transport (Shalby et al., 2020). Wind may also contribute external phosphorus inputs through atmospheric dust deposition (Brahney et al., 2014). It may also reinforce diatom dominance by dissipating smaller, stratification-adapted groups (Kahru et al., 1993). However, the consistent diatom dominance suggests that wind modulates bloom magnitude, but its effect remains relatively limited in reshaping community structure.

Rainfall also exerted a significant influence, with a strong positive effect on picoeukaryotes and the synergized effect with wind to promote fucoxanthin. This reflects mechanisms such as enhancing nutrient availability through watershed runoff and water-column mixing (Goberville et al., 2010; Valenti et al., 2016; De Oliveira et al., 2023; Grossi et al., 2024).

Similar climate-driven dynamics have been reported in other oligotrophic Mediterranean lagoons, including Ria Formosa, Els Alfacs, and Ayrolle (Bec et al., 2011; Derolez et al., 2019; Rodrigues et al., 2021).

Climatic variables significantly contribute to explaining phytoplankton variability, although their importance strongly differed among lagoons. In eu-hypertrophic lagoons such as Biguglia and Palo, recurrent nutrient peaks strongly constrained phytoplankton dynamics, making climatic influences comparatively weak and less detectable. Conversely, in oligotrophic lagoons like Diana and Urbino, climatic control became more visible and influential, likely because the weaker nutrient forcing enhances the role of climate, which indirectly affects phytoplankton through impacts on water-column stability and nutrient delivery and availability (Stefanova et al., 2019). Under nutrient limitation, climate-driven processes can mimic anthropogenic nutrient inputs, but at a much lower magnitude, as nutrient concentrations and phytoplankton abundances remain low, sustaining their oligotrophic status (Bec et al., 2011; Derolez et al., 2019; Rodrigues et al., 2021). These results suggest a hierarchical interaction, where nutrient control prevails and masks the influence of climate when both drivers are present, while climate becomes a more influential forcing under low nutrient pressure (Alvarez-Cobelas et al., 2019). This interpretation aligns with Newton et al. (2020), who showed that nutrient enrichment induces immediate ecological responses, whereas climatic forcing exerts more diffuse effects that become apparent only when nutrient concentrations are low. In such nutrient-limited environments, phytoplankton communities are typically adapted to scarcity and respond weakly to strong nutrient enrichment (Leruste et al., 2019), which enhances the importance of moderate climate-driven effects on their dynamics.

But interestingly, relative size-class pigment contributions (micro versus nano-picophytoplankton) did not differ consistently between sites in relation to physicochemical gradients and showed weak associations with climatic variables. This suggests either that climate exerts an influence on size-class competition independently of nutrient conditions or that taxa within the same size class respond differently to nutrient control. It may also reflect that species within each size-class and taxonomic group differ between sites. In Diana and Urbino, the stable dominance of fucoxanthin reflects communities of small diatoms adapted to oligotrophic and stable water-column conditions (Leruste et al., 2019). In contrast, Biguglia and Palo may host opportunistic diatom species that respond to nutrient pulses (Ligorini et al., 2022a), with an additional alternation between diatom and dinoflagellate dominance likely linked to the hydrodynamic variability in these systems (Garrido et al., 2016). However, pigment contents vary among taxa and with environmental conditions (Yang et al., 2024), thereby limiting the interpretation of pigment data.

The higher nutrient exposure observed in Biguglia and Palo, including more frequent and more intense nutrient peaks compared to Diana and Urbino, likely explains the stronger nutrient control and may be driven by several factors. In Biguglia, recurrent and substantial anthropogenic inputs from the strong urbanized watershed likely contribute to nutrient enrichment (90 Mm3 per year of freshwater; Garrido et al., 2016). In Palo, some sources of nutrient inputs (air base and commercial area), frequent closures of the sea channel, a high watershed-to-lagoon surface ratio, and the presence of surrounding wetlands (AERMC, 2021) may create conditions favoring nutrient retention (Bec et al., 2011). In both systems, nutrient-rich sediments increase the risk of sedimentary release, thereby reinforcing internal nutrient loading within the lagoon (Shalby et al., 2020; Zennaro et al., 2024). These features are consistent with an increased risk of nutrient accumulation and retention, which can frequently trigger phytoplankton responses (Sathicq et al., 2017; Minicheva et al., 2018; Derolez et al., 2020). By contrast, Diana and Urbino seem to be less exposed to nutrient pressures. Their watersheds are minimally anthropized and receive only sparse agricultural inputs, although agricultural activity is slightly less developed around Diana (AERMC, 2021). Their deep and tectonic morphology promotes dilution, reducing nutrient accumulation in the surface layer. Internal nutrient release is also limited: Diana's sediments are nutrient-poor (AERMC, 2021), and shellfish farming further limits nutrient availability by consuming part of the released nutrients (Le Ray et al., 2023), whereas Urbino's sediments are richer but likely stabilized by *Cymodocea nodosa* seagrass meadows (Garrido et al., 2016; Ligorini et al., 2022a). These factors may explain the low frequency and intensity of nutrient pulses and reduce nutrient control.

However, nutrient and climatic influences may still be underestimated in our study, which could explain why not all phytoplankton variability was accounted for. Nutrient data were based on single-day water column measurements, potentially missing enrichment events due to dilution or biological uptake. Similarly, despite the selection of climatic variables and use of optimized temporal windows, part of the climate signal may have been overlooked. As the analysis focuses on the summer period in a Mediterranean climate, when rainfall is scarce, precipitation effects are likely underestimated and would probably be more impactful in other seasons. Refining climatic metrics across complementary timescales and seasons could improve our understanding of multi-scale climate impacts (Adrian et al., 2012).

Additional drivers not quantified may also shape phytoplankton dynamics and contribute to differences observed among lagoons. Zooplankton composition and grazing strategies, although not quantified in our study, are shaped by the composition and abundances of

phytoplankton communities, but also by nutrient sources, mixing conditions (Pomati et al., 2020; To et al., 2025), and temperature, which can enhance grazing activity (Oviatt, 2004; Berger et al., 2006). Consequently, variations in zooplankton composition and grazing pressure, whether driven by phytoplankton or environmental factors, are likely to have, in turn, constrained the observed phytoplankton dynamics (Bi et al., 2021).

Macrophytes also influence phytoplankton dynamics through competition for nutrients, and seagrass meadows enhance sediment stabilization and water clarity, thereby constraining phytoplankton development (Garrido et al., 2016; Le Fur et al., 2018). The composition of macrophyte communities differs among lagoons: while *Cymodocea nodosa* meadows dominate in Diana and Urbino (with lower total coverage in Diana) (Ligorini et al., 2022a), Palo and Biguglia are characterized by variable *Ruppia cirrhosa* stands, sometimes replaced by *Zostera noltei* in Palo or *Stuckenia pectinata* in Biguglia, and occasionally by macroalgal dominance (Pasqualini et al., 2017; Ligorini et al., 2022b). The co-occurrence of unstable macrophyte patterns and high phytoplankton variability in Biguglia and Palo suggests shared environmental drivers and reciprocal interactions between compartments.

4.3. Toward a global climate-driven shift in lagoon ecological functioning

As climate change progresses, climate forcing could gain importance in shaping phytoplankton temporal trends and even trajectories, with global warming becoming a predominant force in coastal lagoons (Talavera et al., 2024). Oligotrophic systems provide suitable conditions to detect early signals, acting as sentinels of climate change (Stefanova et al., 2019). By contrast, the shift from nutrient to climate control may be most evident in historically eutrophicated lagoons undergoing restoration, where nutrient availability increasingly depends on climate-driven inputs, potentially altering both the timing and origin of nutrient supply. An accelerated shift is possible since the combination of warming and nutrient scarcity can reduce phytoplankton thermal tolerance and increase their ecological vulnerability to environmental changes (Thomas et al., 2017; Pomati et al., 2020; Bi et al., 2021). Early signs of such climate-driven ecological shifts are already observed in other eutrophised Mediterranean coastal systems: in the Ria de Aveiro, reduced freshwater inflows and rising temperatures have led to increased salinity and reduced Chlorophyll *a* concentrations (Lloret et al., 2008; Lopes et al., 2019) and in the Venice lagoon, nutrient reductions have promoted cyanobacterial dominance (Pesce et al., 2018).

Our results also suggest that different climatic drivers exert distinct but yet complementary effects: air temperature favored warm-adapted taxa such as phycoerythrin-rich picocyanobacteria, which may explain the recent sustained values of the nano-picophytoplankton size class ratio, whereas wind and rainfall supported larger or nutrient competitive groups such as diatoms and picoeukaryotes. These drivers operate through different processes: warming may promote stratification and enhance phosphorus release from sediments, while wind and precipitation favor mixing and nutrient delivery from the watershed (Winder and Sommer, 2012; Zaldívar et al., 2008; Lopes et al., 2019; Shalby et al., 2020). This coexistence of opposing yet complementary forces sustains functional diversity (Goberville et al., 2010; Wang et al., 2025). But future projections of intensified warming and prolonged droughts in Mediterranean regions (MWO, 2018; Ligorini et al., 2022b; Guzmán et al., 2023; Macias et al., 2025), with declining freshwater availability and projected reduction in summer rainfall (Pesce et al., 2018), may reduce this climate variability and promote community homogenization under warming (Vereshchaka et al., 2023).

In our study, climatic changes do not yet appear sufficiently linear and impactful to produce visible effects on lagoon trajectories. Yet, climate modulates physicochemical patterns and may progressively drive lagoon functioning in the future. Some aspects deserve particular attention, as they may become increasingly affected by climate change in the future. Phosphorus may become more available through warming-enhanced internal recycling (Zennaro et al., 2024). Salinity is also likely to be reshaped (Da Costa et al., 2022; Talavera et al., 2024): it may increase in summer due to evaporation, reduced rainfall, and lower river inflows (Levang and Schmitt, 2015; Pesce et al., 2018; Shalby et al., 2020), while intense rainfall, runoff, or seawater intrusion may conversely reduce it or induce rapid fluctuations (Jiang et al., 2022; De Oliveira et al., 2023). The stability of the water column, which regulates nutrient resupply, suspended particulate matter, and light penetration, may be particularly affected during the summer period (Cloern, 1999; Da Costa et al., 2022). With global warming, an increase in the occurrence and intensity of stratified phases is expected (Pomati et al., 2020; Vereshchaka et al., 2023). The maintenance of seawater exchanges also appears crucial, as they regulate both nutrient and climatic effects (Cecchi et al., 2016; Rodrigues et al., 2021; Ligorini et al., 2022b). As emphasized by the 2010 eutrophication crisis in Palo, triggered by the absence of summer channel opening combined with extreme warming, and by the reduced eutrophication observed in the sea-connected part of Biguglia, water exchanges and effective grau management can mitigate nutrient stress. Yet these exchanges may themselves be altered, both by the current tendency toward channel closure in these lagoons and, in the longer term, by sea-level rise (Lopes et al., 2019; Guzmán et al., 2023; IPCC, 2023). In addition, climate forcing may progressively reorganize taxonomic groups, including the disruption of diatom-dinoflagellate competition through direct and indirect effects (Garrido et al., 2016; Pesce et al., 2018; Bi et al., 2021) or the expansion of warm-adapted and grazing-tolerant taxa such as picocyanobacteria at the expense of picoeukaryotes (Oviatt, 2004; Collos et al., 2009; Bec et al., 2011; Pomati et al., 2020; Leruste et al., 2021).

Since temporal trends and ecological responses to environmental drivers differ between lagoons, anticipating and managing these potential changes requires refining our understanding of site-specific functioning and vulnerabilities (Zaldívar et al., 2008; Derolez et al., 2019) to implement adaptive management strategies (Sathicq et al., 2017; Stefanova et al., 2019) tailored to each lagoon's context.

CRediT authorship contribution statement

Aurore Moulin: Writing – original draft, Visualization, Methodology, Investigation, Formal analysis, Data curation. **Béatrice Bec:** Writing – review & editing, Writing – original draft, Resources, Methodology, Conceptualization. **Olivier Boutron:** Writing – review & editing, Validation, Supervision, Methodology. **Valérie Derolez:** Writing – review & editing, Validation, Methodology, Investigation, Formal analysis, Data curation. **Marie Garrido:** Writing – review & editing, Resources. **Vanina Pasqualini:** Writing – review & editing, Supervision, Project administration, Investigation. **Nathalie Malet:** Writing – review & editing, Visualization, Validation, Supervision, Project administration, Investigation, Funding acquisition, Conceptualization.

Declaration of Generative AI and AI-assisted technologies in the writing process

During the preparation of this work the author(s) used ChatGPT (OpenAI) in order to improve readability and language. After using this tool/service, the author(s) reviewed and edited the content as needed and take(s) full responsibility for the content of the publication.

Declaration of competing interest

The authors declare the following financial interests/personal relationships which may be considered as potential competing interests: Aurore MOULIN reports financial support was provided by French National Research Agency. If there are other authors, they declare that they have no known competing financial interests or personal relationships that could have appeared to influence the work reported in this paper.

Acknowledgements

Aurore Moulin was awarded a grant by the Corsican Regional Council and the University of Corsica. Her PhD was co-financed equally (50 %) by the University of Corsica and Ifremer. This study was based on data collected during the projects LMN, OBSLAG and Water Framework Directive, which received financial support from Ifremer and Agence de l'Eau Rhône Méditerranée Corse. This study was supported by funding from the French Government and the National Research Agency (ANR-22-EXES-0016).

The authors are extremely grateful to Martine Fortuné, Elodie Foucault, and Grégory Messiaen for the analyses of nutrients and to Elise Hatey for the analyses of HPLC during all the years of the monitoring program. We thank our colleagues from Ifremer LEROC, LERPAC, and LERPAC-Corse.

Appendix A. Supplementary data

Supplementary data to this article can be found online at https://doi.org/10.1016/j.marpolbul.2025.119080.

Data availability

Data will be made available on request.

References

Adrian, R., Gerten, D., Huber, V., Wagner, C., Schmidt, S.R., 2012. Windows of change: temporal scale of analysis is decisive to detect ecosystem responses to climate change. Mar. Biol. 159, 2533–2542. https://doi.org/10.1007/s00227-012-1938-1.

AERMC (Agence de l'eau Rhône Méditerranée Corse), 2021. Valorisation des données des lagunes de la façade méditerranéenne continentale : analyse des tendances d'évolution et identification des facteurs de pression. Rapport technique 124.

Alvarez-Cobelas, M., Rojo, C., Benavent-Corai, J., 2019. Long-term phytoplankton dynamics in a complex temporal realm. Sci. Rep. 9, 15967. https://doi.org/10.1038/s41598-019-52333-z.

Bailey, L.D., Pol, M. van de, 2016. climwin: An R Toolbox for Climate Window Analysis. PLoS One 11, e0167980. https://doi.org/10.1371/journal.pone.0167980.

Bec, B., Collos, Y., Souchu, P., Vaquer, A., Lautier, J., Fiandrino, A., Benau, L., Orsoni, V., Laugier, T., 2011. Distribution of picophytoplankton and nanophytoplankton along an anthropogenic eutrophication gradient in French Mediterranean coastal lagoons. Aquat. Microb. Ecol. 63, 29–45. https://doi.org/10.3354/ame01480.

Berger, S.A., Diehl, S., Stibor, H., Trommer, G., Ruhenstroth, M., Wild, A., Weigert, A., Jäger, C.G., Striebel, M., 2006. Water temperature and mixing depth affect timing and magnitude of events during spring succession of the plankton. Oecologia 150, 643–654. https://doi.org/10.1007/s00442-006-0550-9.

Bi, R., Cao, Z., Ismar-Rebitz, S.M.H., Sommer, U., Zhang, H., Ding, Y., Zhao, M., 2021. Responses of marine diatom-dinoflagellate competition to multiple environmental drivers: abundance, elemental, and biochemical aspects. Front. Microbiol. 12. https://doi.org/10.3389/fmicb.2021.731786.

Bird, E.C.F., 2011. Coastal Geomorphology: An Introduction. Wiley.

Brahney, J., Ballantyne, A.P., Kociolek, P., Spaulding, S., Otu, M., Porwoll, T., Neff, J.C., 2014. Dust mediated transfer of phosphorus to alpine lake ecosystems of the Wind River Range, Wyoming, USA. Biogeochemistry 120, 259–278. https://doi.org/10.1007/s10533-014-9994-x.

Cecchi, P., Garrido, M., Collos, Y., Pasqualini, V., 2016. Water flux management and phytoplankton communities in a Mediterranean coastal lagoon. Part II: Mixotrophy of dinoflagellates as an adaptive strategy? Mar. Pollut. Bull. 108, 120–133. https://doi.org/10.1016/j.marpolbul.2016.04.041.

Chen, W., Wang, X., Yang, S., 2023. Response of phytoplankton community structure to environmental changes in the coastal areas of northern China. Mar. Pollut. Bull. 195, 115300. https://doi.org/10.1016/j.marpolbul.2023.115300.

Cloern, J.E., 1999. The relative importance of light and nutrient limitation of phytoplankton growth: a simple index of coastal ecosystem sensitivity to nutrient enrichment. Aquat. Ecol. 33, 3–15. https://doi.org/10.1023/A:1009952125558.

Collos, Y., Bec, B., Jauzein, C., Abadie, E., Laugier, T., Lautier, J., Pastoureaud, A., Souchu, P., Vaquer, A., 2009. Oligotrophication and emergence of picocyanobacteria and a toxic dinoflagellate in Thau lagoon, southern France. J. Sea Res. 61, 68–75. https://doi.org/10.1016/j.seares.2008.05.008.

Da Costa, Á.K.R., Pereira, L.C.C., Jiménez, J.A., De Oliveira, A.R.G., De Jesus Flores-Montes, M., Da Costa, R.M., 2022. Effects of extreme climatic events on the hydrological parameters of the estuarine waters of the Amazon Coast. Estuar. Coasts 45, 1517–1533. https://doi.org/10.1007/s12237-022-01056-y.

David, M., Bailly-Comte, V., Munaron, D., Fiandrino, A., Stieglitz, T.C., 2019. Groundwater discharge to coastal streams – a significant pathway for nitrogen inputs to a hypertrophic Mediterranean coastal lagoon. Sci. Total Environ. 677, 142–155. https://doi.org/10.1016/j.scitotenv.2019.04.233.

De Oliveira, A.R.G., Queiroz, J.B.M., Pardal, E.C., Pereira, L.C.C., Da Costa, R.M., 2023. How does the phytoplankton community respond to the effects of La Niña and post-drought events in a tide-dominated Amazon estuary? Aquat. Sci. 85, 9. https://doi.org/10.1007/s00027-022-00904-0.

Derolez, V., Bec, B., Munaron, D., Fiandrino, A., Pete, R., Simier, M., Souchu, P., Laugier, T., Aliaume, C., Malet, N., 2019. Recovery trajectories following the reduction of urban nutrient inputs along the eutrophication gradient in French Mediterranean lagoons. Ocean Coast. Manag. 171, 1–10. https://doi.org/10.1016/j.ocecoaman.2019.01.012.

Derolez, V., Soudant, D., Malet, N., Chiantella, C., Richard, M., Abadie, E., Aliaume, C., Bec, B., 2020. Two decades of oligotrophication: evidence for a phytoplankton community shift in the coastal lagoon of Thau (Mediterranean Sea, France). Estuar. Coast. Shelf Sci. 241, 106810. https://doi.org/10.1016/j.ecss.2020.106810.

Doré, H., Leconte, J., Guyet, U., Breton, S., Farrant, G.K., Demory, D., Ratin, M., Hoebeke, M., Corre, E., Pitt, F.D., Ostrowski, M., Scanlan, D.J., Partensky, F., Six, C., Garczarek, L., 2022. Global phylogeography of marine Synechococcus in coastal areas reveals strong community shifts. mSystems 7, e0065622. https://doi.org/10.1128/msystems.00656-22.

D'ors, A., Bartolomé, M.C., Sánchez-Fortún, S., 2016. Repercussions of salinity changes and osmotic stress in marine phytoplankton species. Estuar. Coast. Shelf Sci. 175, 169–175. https://doi.org/10.1016/j.ecss.2016.04.004.

Dray, S., Dufour, A.-B., Thioulouse, J., 2002. ade4: Analysis of Ecological Data: Exploratory and Euclidean Methods in Environmental Sciences. CRAN: Contributed Packages. https://doi.org/10.32614/cran.package.ade4.

Eisenreich, S., Bernasconi, C., Campostrini, P., de Roo, A., George, G., Heiskanen, A., Hjorth, J., Hoepffner, N., Jones, K., Noges, P., Pirrone, N., Runnalls, N., Somma, F., Stilanakis, N., Umlauf, G., van de Bund, W., Viaroli, P., Vogt, J., Zaldivar, J., Cornell, S., 2005. Climate Change and the European Water Dimension. Recommendations and Key Findings. European Commission.

Field, C.B., Behrenfeld, M.J., Randerson, J.T., Falkowski, P., 1998. Primary production of the biosphere: integrating terrestrial and oceanic components. Science 281, 237–240. https://doi.org/10.1126/science.281.5374.237.

Garrido, M., Cecchi, P., Collos, Y., Agostini, S., Pasqualini, V., 2016. Water flux management and phytoplankton communities in a Mediterranean coastal lagoon. Part I: how to promote dinoflagellate dominance? Mar. Pollut. Bull. 104, 139–152. https://doi.org/10.1016/j.marpolbul.2016.01.049.

Giorgi, F., 2006. Climate change hot-spots. Geophys. Res. Lett. 33, 2006GL025734. https://doi.org/10.1029/2006GL025734.

Goberville, E., Beaugrand, G., Sautour, B., Tréguer, P., Somlit, T., 2010. Climate-driven changes in coastal marine systems of western Europe. Mar. Ecol. Prog. Ser. 408, 129–147. https://doi.org/10.3354/meps08564.

Grébert, T., Doré, H., Partensky, F., Farrant, G.K., Boss, E.S., Picheral, M., Guidi, L., Pesant, S., Scanlan, D.J., Wincker, P., Acinas, S.G., Kehoe, D.M., Garczarek, L., 2018. Light color acclimation is a key process in the global ocean distribution of *Synechococcus cyanobacteria*. Proc. Natl. Acad. Sci. U.S.A. 115. https://doi.org/10.1073/pnas.1717069115.

Grossi, F., Lagasio, M., Napoli, A., Provenzale, A., Tepsich, P., 2024. Phytoplankton spring bloom in the NW Mediterranean Sea under climate change. Sci. Total Environ. 914, 169884. https://doi.org/10.1016/j.scitotenv.2024.169884.

Guzmán, O., Mendoza, E., van Tussenbroek, B.I., Silva, R., 2023. Effects of climate-change-related phenomena on coastal ecosystems in the Mexican Caribbean. Sustainability 15, 12042. https://doi.org/10.3390/su151512042.

IPCC, 2023. Climate change 2023: synthesis report. In: Team, Core Writing, Lee, H., Romero, J. (Eds.), Contribution of Working Groups I, II and III to the Sixth Assessment Report of the Intergovernmental Panel on Climate Change. IPCC, Geneva, Switzerland. https://doi.org/10.59327/IPCC/AR6-9789291691647. Intergovernmental Panel on Climate Change (IPCC).

Jeppesen, E., Søndergaard, M., Meerhoff, M., Lauridsen, T.L., Jensen, J.P., 2007. Shallow lake restoration by nutrient loading reduction—some recent findings and challenges ahead. Hydrobiologia 584, 239–252. https://doi.org/10.1007/s10750-007-0596-7.

Jiang, T., Wu, G., Niu, P., Cui, Z., Bian, X., Xie, Y., Shi, H., Xu, X., Qu, K., 2022. Short-term changes in algal blooms and phytoplankton community after the passage of Super Typhoon Lekima in a temperate and inner sea (Bohai Sea) in China. Ecotoxicol. Environ. Saf. 232, 113223. https://doi.org/10.1016/j.ecoenv.2022.113223.

Kahru, M., Leppanen, J.-M., Rud, O., 1993. Cyanobacterial blooms cause heating of the sea surface. Mar. Ecol. Prog. Ser. 101, 1–7. https://doi.org/10.3354/meps101001.

La Jeunesse, I., Cirelli, C., Sellami, H., Aubin, D., Deidda, R., Baghdadi, N., 2015. Is the governance of the Thau coastal lagoon ready to face climate change impacts? Ocean Coast. Manag. 118, 234–246. https://doi.org/10.1016/j.ocecoaman.2015.05.014.

Le Fur, I., De Wit, R., Plus, M., Oheix, J., Derolez, V., Simier, M., Nathalie, M., Ouisse, V., 2018. Re-oligotrophication trajectories of macrophyte assemblages in Mediterranean coastal lagoons studied from 17-years' time-series. Mar. Ecol. Prog. Ser. 608. https://doi.org/10.3354/meps12814.

Le Ray, J., Bec, B., Fiandrino, A., Lagarde, F., Cimiterra, N., Raimbault, P., Roques, C., Rigaud, S., Régis, J., Mostajir, B., Mas, S., Richard, M., 2023. Impact of anoxia and oyster mortality on nutrient and microbial planktonic components: a mesocosm study. Aquaculture 566, 739171. https://doi.org/10.1016/j.aquaculture.2022.739171.

Leruste, A., Malet, N., Munaron, D., Derolez, V., Hatey, E., Collos, Y., De Wit, R., Bec, B., 2016. First steps of ecological restoration in Mediterranean lagoons: shifts in phytoplankton communities. Estuar. Coast. Shelf Sci. 180, 190–203. https://doi.org/10.1016/j.ecss.2016.06.029.

Leruste, A., Pasqualini, V., Garrido, M., Malet, N., De Wit, R., Bec, B., 2019. Physiological and behavioral responses of phytoplankton communities to nutrient availability in a

disturbed Mediterranean coastal lagoon. Estuar. Coast. Shelf Sci. 219, 176–188. https://doi.org/10.1016/j.ecss.2019.02.014.
Leruste, A., Garrido, M., Malet, N., Bec, B., De Wit, R., Cecchi, P., Pasqualini, V., 2021. Impact of nutrient availability on the trophic strategies of the planktonic protist communities in a disturbed Mediterranean coastal lagoon. Hydrobiologia 848, 1101–1119. https://doi.org/10.1007/s10750-021-04517-w.
Levang, S.J., Schmitt, R.W., 2015. Centennial changes of the global water cycle in CMIP5 models. J. Clim. 28, 6489–6502.
Ligorini, V., Malet, N., Garrido, M., Derolez, V., Amand, M., Bec, B., Cecchi, P., Pasqualini, V., 2022a. Phytoplankton dynamics and bloom events in oligotrophic Mediterranean lagoons: seasonal patterns but hazardous trends. Hydrobiologia 849, 2353–2375. https://doi.org/10.1007/s10750-022-04874-0.
Ligorini, V., Malet, N., Garrido, M., Four, B., Etourneau, S., Leoncini, A.S., Dufresne, C., Cecchi, P., Pasqualini, V., 2022b. Long-term ecological trajectories of a disturbed Mediterranean coastal lagoon (Biguglia lagoon): ecosystem-based approach and considering its resilience for conservation? Front. Mar. Sci. 9, 937795. https://doi.org/10.3389/fmars.2022.937795.
Ligorini, V., Garrido, M., Malet, N., Simon, L., Alonso, L., Bastien, R., Aiello, A., Cecchi, P., Pasqualini, V., 2023. Response of phytoplankton communities to variation in salinity in a small Mediterranean coastal lagoon: future management and foreseen climate change consequences. Water 15, 3214. https://doi.org/10.3390/w15183214.
Venice system for the classification of marine waters according to salinity. Limnol. Oceanogr. 3, 1958, 346–347. https://doi.org/10.4319/lo.1958.3.3.0346.
Lloret, J., Marín, A., Marín-Guirao, L., 2008. Is coastal lagoon eutrophication likely to be aggravated by global climate change? Estuar. Coast. Shelf Sci. 78, 403–412. https://doi.org/10.1016/j.ecss.2008.01.003.
Lopes, J.F., Lopes, C.L., Dias, J.M., 2019. Climate change impact in the Ria de Aveiro Lagoon ecosystem: a case study. JMSE 7, 352. https://doi.org/10.3390/jmse7100352.
Macias, D., Bisselink, B., Carmona-Moreno, C., Druon, J.-N., Duteil, O., Garcia-Gorriz, E., Grizzetti, B., Guillen, J., Miladinova, S., Pistocchi, A., Piroddi, C., Polimene, L., Serpetti, N., Stips, A., Trichakis, I., Udias, A., Vigiak, O., 2025. The overlooked impacts of freshwater scarcity on oceans, as evidenced by the Mediterranean Sea. Nat. Commun. 16, 998. https://doi.org/10.1038/s41467-024-54979-4.
Margalef, R., 1978. Life-forms of phytoplankton as survival alternatives in an unstable environment. Oceanol. Acta 1, 493–509.
Mark Jr., H., J.W, 2015. Optimizing the Regression Model: The Challenge of Intercept–Bias and Slope "Correction". Spectroscopy-07-01-2015 30, pp. 32–37, 48.
Mediterranean Wetlands Observatory (MWO), 2018. Mediterranean Wetlands Outlook 2: Solutions for sustainable Mediterranean wetlands. Tour du Valat, France, p. 148.
Minicheva, G.G., Bolshakov, V.N., Kalashnik, E.S., Zotov, A.B., Marinets, A.V., 2018. Assessment of the reactions of algal communities to influence of climatic factors in the North-Western Black Sea ecosystem. Inter. J. Algae 20, 121–134. https://doi.org/10.1615/InterJAlgae.v20.i2.20.
Newton, A., Brito, A.C., Icely, J.D., Derolez, V., Clara, I., Angus, S., Schernewski, G., Inácio, M., Lillebø, A.I., Sousa, A.I., Béjaoui, B., Solidoro, C., Tosic, M., Cañedo-Argüelles, M., Yamamuro, M., Reizopoulou, S., Tseng, H.-C., Canu, D., Roselli, L., Maanan, M., Cristina, S., Ruiz-Fernández, A.C., Lima, R.F.D., Kjerfve, B., Rubio-Cisneros, N., Pérez-Ruzafa, A., Marcos, C., Pastres, R., Pranovi, F., Snoussi, M., Turpie, J., Tuchkovenko, Y., Dyack, B., Brookes, J., Povilanskas, R., Khokhlov, V., 2018. Assessing, quantifying and valuing the ecosystem services of coastal lagoons. J. Nat. Conserv. 44, 50–65. https://doi.org/10.1016/j.jnc.2018.02.009.
Newton, A., Icely, J., Cristina, S., Perillo, G.M.E., Turner, R.E., Ashan, D., Cragg, S., Luo, Y., Tu, C., Li, Y., Zhang, H., Ramesh, R., Forbes, D.L., Solidoro, C., Béjaoui, B., Gao, S., Pastres, R., Kelsey, H., Taillie, D., Nhan, N., Brito, A.C., de Lima, R., Kuenzer, C., 2020. Anthropogenic, direct pressures on coastal wetlands. Front. Ecol. Evol. 8. https://doi.org/10.3389/fevo.2020.00144.
Orsoni, V., Souchu, P., Sauzade, D., 2001. Caractérisation de l'état d'eutrophisation des trois principaux étangs corses (Biguglia, Diana et Urbino), et proposition de renforcement de leur surveillance.
Ouaissa, S., Gómez-Jakobsen, F., Yebra, L., Ferrera, I., Moreno-Ostos, E., Belando, M.D., Ruiz, J.M., Mercado, J.M., 2023. Phytoplankton dynamics in the Mar Menor, a Mediterranean coastal lagoon strongly impacted by eutrophication. Mar. Pollut. Bull. 192, 115074. https://doi.org/10.1016/j.marpolbul.2023.115074.
Oviatt, C.A., 2004. The changing ecology of temperate coastal waters during a warming trend. Estuaries 27, 895–904. https://doi.org/10.1007/BF02803416.
Pasqualini, V., Derolez, V., Garrido, M., Orsoni, V., Baldi, Y., Etourneau, S., Leoni, V., Rébillout, P., Laugier, T., Souchu, P., Malet, N., 2017. Spatiotemporal dynamics of submerged macrophyte status and watershed exploitation in a Mediterranean coastal lagoon: understanding critical factors in ecosystem degradation and restoration. Ecol. Eng. 102, 1–14. https://doi.org/10.1016/j.ecoleng.2017.01.027.
Pérez-Ruzafa, A., Marcos, C., Pérez-Ruzafa, I.M., Pérez-Marcos, M., 2011. Coastal lagoons: "transitional ecosystems" between transitional and coastal waters. J. Coast. Conserv. 15, 369–392. https://doi.org/10.1007/s11852-010-0095-2.
Pesce, M., Critto, A., Torresan, S., Giubilato, E., Santini, M., Zirino, A., Ouyang, W., Marcomini, A., 2018. Modelling climate change impacts on nutrients and primary production in coastal waters. Sci. Total Environ. 628–629, 919–937. https://doi.org/10.1016/j.scitotenv.2018.02.131.
Pohlert, T., 2023. trend: Non-Parametric Trend Tests and Change-Point Detection. https://CRAN.R-project.org/package=trend.
Pomati, F., Shurin, J.B., Andersen, K.H., Tellenbach, C., Barton, A.D., 2020. Interacting temperature, nutrients and zooplankton grazing control phytoplankton size-abundance relationships in eight Swiss lakes. Front. Microbiol. 10. https://doi.org/10.3389/fmicb.2019.03155.
R Core Team, 2024. R: A Language and Environment for Statistical Computing. R Foundation for Statistical Computing, Vienna, Austria. https://www.R-project.org/.
Rodrigues, M., Rosa, A., Cravo, A., Jacob, J., Fortunato, A.B., 2021. Effects of climate change and anthropogenic pressures in the water quality of a coastal lagoon (Ria Formosa, Portugal). Sci. Total Environ. 780, 146311. https://doi.org/10.1016/j.scitotenv.2021.146311.
Roy, S., Llewellyn, C.A., Egeland, E.S., Johnsen, G., 2011. Phytoplankton Pigments: Characterization, Chemotaxonomy and Applications in Oceanography. Cambridge University Press, Cambridge.
Sabater, S., Freixa, A., Jiménez, L., López-Doval, J., Pace, G., Pascoal, C., Perujo, N., Craven, D., González-Trujillo, J.D., 2023. Extreme weather events threaten biodiversity and functions of river ecosystems: evidence from a meta-analysis. Biol. Rev. 98, 450–461. https://doi.org/10.1111/brv.12914.
Sathicq, M.B., Gómez, N., Bauer, D.E., Donadelli, J., 2017. Use of phytoplankton assemblages to assess the quality of coastal waters of a transitional ecosystem: Río de la Plata estuary. Cont. Shelf Res. 150, 10–17. https://doi.org/10.1016/j.csr.2016.08.009.
Sen, P.K., 1968. Estimates of the regression coefficient based on Kendall's Tau. J. Am. Stat. Assoc. 63, 1379–1389. https://doi.org/10.1080/01621459.1968.10480934.
Shalby, A., Elshemy, M., Zeidan, B.A., 2020. Assessment of climate change impacts on water quality parameters of Lake Burullus, Egypt. Environ. Sci. Pollut. Res. 27, 32157–32178. https://doi.org/10.1007/s11356-019-06105-x.
Souchu, P., Bec, B., Smith, V.H., Laugier, T., Fiandrino, A., Benau, L., Orsoni, V., Collos, Y., Vaquer, A., 2010. Patterns in nutrient limitation and chlorophyll *a* along an anthropogenic eutrophication gradient in French Mediterranean coastal lagoons. Can. J. Fish. Aquat. Sci. 67, 743–753. https://doi.org/10.1139/F10-018.
Stefanova, A., Hesse, C., Krysanova, V., Volk, M., 2019. Assessment of socio-economic and climate change impacts on water resources in four European lagoon catchments. Environ. Manag. 64, 701–720. https://doi.org/10.1007/s00267-019-01188-1.
Tagliapietra, D., Sigovini, M., Ghirardini, A.V., 2009. A review of terms and definitions to categorise estuaries, lagoons and associated environments. Mar. Freshw. Res. 60, 497. https://doi.org/10.1071/MF08088.
Talavera, L., Domínguez-Gómez, J.A., Navarro, N., Rodríguez-Santalla, I., 2024. Analysing spatiotemporal variability of chlorophyll-a concentration and water surface temperature in coastal lagoons of the Ebro Delta (NW Mediterranean Sea, Spain). JMSE 12, 941. https://doi.org/10.3390/jmse12060941.
Thomas, M.K., Aranguren-Gassis, M., Kremer, C.T., Gould, M.R., Anderson, K., Klausmeier, C.A., Litchman, E., 2017. Temperature–nutrient interactions exacerbate sensitivity to warming in phytoplankton. Glob. Chang. Biol. 23, 3269–3280. https://doi.org/10.1111/gcb.13641.
To, S.-W., Acevedo-Trejos, E., Smith, S.L., Chakraborty, S., Merico, A., 2025. Ecological and environmental factors influencing exclusion patterns of phytoplankton size classes in lake systems. Ecol. Complex. 61, 101115. https://doi.org/10.1016/j.ecocom.2024.101115.
Tuchkovenko, Y., Khokhlov, V., Loboda, N., 2023. Climate change impact on the freshwater balance of quasi-closed lagoons in the North-Western Black Sea coast. J. Water Clim. Chang. 14, 2416–2431. https://doi.org/10.2166/wcc.2023.109.
Valenti, D., Denaro, G., Spagnolo, B., Mazzola, S., Basilone, G., Conversano, F., Brunet, C., Bonanno, A., 2016. Stochastic models for phytoplankton dynamics in Mediterranean Sea. Ecol. Complex. 27, 84–103. https://doi.org/10.1016/j.ecocom.2015.06.001.
Vanselow, A., Halekotte, L., Pal, P., Wieczorek, S., Feudel, U., 2022. Rate-induced Tipping Can Trigger Plankton Blooms. https://doi.org/10.48550/arXiv.2212.01244.
Vereshchaka, A.L., Mikaelyan, A.S., Piontkovski, S.A., Lunina, A.A., 2023. A mesoplankton biomass decline in the Central Atlantic coupled with an increase of surface temperature and an expansion of low-productive zones. Glob. Ecol. Biogeogr. 32, 1365–1376. https://doi.org/10.1111/geb.13703.
Vidal, J.-P., Martin, E., Franchistéguy, L., Baillon, M., Soubeyroux, J.-M., 2010. A 50-year high-resolution atmospheric reanalysis over France with the Safran system. Int. J. Climatol. 30, 1627–1644. https://doi.org/10.1002/joc.2003.
Wang, X., Wu, X., Sun, J., 2025. Seasonal dynamics and key drivers of phytoplankton community structure in the Eastern Indian Ocean. Mar. Pollut. Bull. 212, 117548. https://doi.org/10.1016/j.marpolbul.2025.117548.
Winder, M., Sommer, U., 2012. Phytoplankton response to a changing climate. Hydrobiologia 698, 5–16. https://doi.org/10.1007/s10750-012-1149-2.
Wood, S., Scheipl, F., 2025. gamm4: Generalized Additive Mixed Models Using "mgcv" and "lme4". https://CRAN.R-project.org/package=gamm4.
Wright, S., Jeffrey, S.W., Mantoura, R., Llewellyn, C., Bjornland, T., Repeta, D., Elschmeyer, N., 1991. Improved HPLC method for the analysis of chlorophylls and carotenoids from marine phytoplankton. Mar. Ecol. Prog. Ser. 77, 183–196. https://doi.org/10.3354/meps077183.
Xu, Y., Xiang, Z., Rizo, E.Z., Naselli-Flores, L., Han, B.-P., 2022. Combination of linear and nonlinear multivariate approaches effectively uncover responses of phytoplankton communities to environmental changes at regional scale. J. Environ. Manag. 305, 114399. https://doi.org/10.1016/j.jenvman.2021.114399.
Yang, L., Cui, Z., Zhang, J., Wang, Hongwei, Wang, Hanbai, Zhang, D., Ding, X., Zha, D., Gao, L., Jiang, T., 2024. Dynamics of phytoplankton assemblages determined by the HPLC–PIGMENTUM approach and the related environmental variables in the northern Chinese sea. Mar. Pollut. Bull. 208, 116999. https://doi.org/10.1016/j.marpolbul.2024.116999.

Zaldívar, J.-M., Cardoso, A.C., Viaroli, P., de Wit, R., Ibañez, C., Reizopoulou, S., Razinkovas, A., Basset, A., Holmer, M., Murray, N., 2008. Eutrophication in Transitional Waters: An Overview.

Zennaro, F., Furlan, E., Canu, D., Alcazar, L.A., Rosati, G., Solidoro, C., Critto, A., 2024. Hypoxia extreme events in a changing climate: Machine learning methods and deterministic simulations for future scenarios development in the Venice Lagoon. Mar. Pollut. Bull. 208, 117028. https://doi.org/10.1016/j.marpolbul.2024.117028.

Zhang, M., Shi, X., Yang, Z., Yu, Y., Shi, L., Qin, B., 2018. Long-term dynamics and drivers of phytoplankton biomass in eutrophic Lake Taihu. Sci. Total Environ. 645, 876–886. https://doi.org/10.1016/j.scitotenv.2018.07.220.